IDIOPATHIC PULMONARY FIBROSIS

The Role of Dimethylarginine Dimethylaminohydrolase in Idiopathic Pulmonary Fibrosis

Soni Savai Pullamsetti,[1,2] Rajkumar Savai,[1,2] Rio Dumitrascu,[2] Bhola Kumar Dahal,[2] Jochen Wilhelm,[2] Melanie Konigshoff,[3] Dariusz Zakrzewicz,[2] Hossein Ardeschir Ghofrani,[2] Norbert Weissmann,[2] Oliver Eickelberg,[3] Andreas Guenther,[2,4] James Leiper,[5] Werner Seeger,[1,2] Friedrich Grimminger,[2] Ralph Theo Schermuly[1,2]*

Idiopathic pulmonary fibrosis (IPF) is a progressive, dysregulated response to alveolar injury that culminates in compromised lung function from excess extracellular matrix production. Associated with high morbidity and mortality, IPF is generally refractory to current pharmacological therapies. We examined fibrotic lungs from mice and from patients with IPF and detected increased expression of dimethylarginine dimethylaminohydrolases (DDAHs)—key enzymes that metabolize asymmetric dimethylarginine (ADMA), which is an endogenous inhibitor of nitric oxide synthase, to form L-citrulline and dimethylamine. DDAHs are up-regulated in primary alveolar epithelial type II cells from these mice and patients where they are colocalized with inducible nitric oxide synthase. In cultured alveolar epithelial type II cells from bleomycin-induced fibrotic mouse lungs, inhibition of DDAH suppressed proliferation and induced apoptosis in an ADMA-dependent manner. In addition, DDAH inhibition reduced collagen production by fibroblasts in an ADMA-independent but transforming growth factor/SMAD–dependent manner. In mice with bleomycin-induced pulmonary fibrosis, the DDAH inhibitor L-291 reduced collagen deposition and normalized lung function. In bleomycin-induced fibrosis, inducible nitric oxide synthase inhibition decreased fibrosis, but an even stronger reduction was observed after inhibition of DDAH. Thus, DDAH inhibition reduces fibroblast-induced collagen deposition in an ADMA-independent manner and reduces abnormal epithelial proliferation in an ADMA-dependent manner, offering a possible therapeutic avenue for attenuation of pulmonary fibrosis.

INTRODUCTION

Among the idiopathic interstitial pneumonias, idiopathic pulmonary fibrosis (IPF) is the most common and aggressive form of lung fibrosis, and its etiology is unidentified. IPF is characterized by recurrent injury of the alveolar epithelium by an unknown cause, modest signs of alveolar inflammation, and profound proliferation of fibroblasts. IPF eventually results in progressive loss of functional alveolar capillary units and lung architecture, as well as scarring of the lung (*1*, *2*). IPF is associated with high morbidity and mortality, and it is generally refractory to currently available pharmacological therapies.

Increased production of nitric oxide (NO) occurs in IPF, likely a result of an increase in inducible NO synthase (iNOS) (*3*–*5*). Mice challenged with bleomycin, a widely used model of pulmonary fibrosis, also exhibit an increase in NO in bronchoalveolar lavage (BAL) fluid (*6*, *7*). However, little is known about the molecular mechanisms that lead to changes in iNOS activity in this disease.

Here, we investigated the role of dimethylarginine dimethylaminohydrolase (DDAH) in the pathogenesis of pulmonary fibrosis. DDAH metabolizes asymmetric dimethylarginine (ADMA) and monomethyl arginine (L-NMMA) to L-citrulline and dimethylamine, which are both endogenous inhibitors of NOS (*8*) (Fig. 1A). To date, two isoforms of DDAH have been identified in mammals, DDAH1 and DDAH2, and they have distinct tissue distributions. DDAH1 is present at highest levels in brain, kidney, pancreas, and liver, whereas DDAH2 is found at high concentrations in fetal tissues, lungs, and highly vascularized tissues (*9*). ADMA and L-NMMA are proteolytic by-products of arginine methylation, a posttranslational modification of arginine carried out by protein arginine methyltransferases (*10*). ADMA and L-NMMA both influence NO signaling (*11*), and the ADMA-DDAH pathway is critical for regulation of NO-mediated cell survival, activation of nuclear factor κB (NFκB), and expression of proinflammatory cytokines (*12*, *13*). Specific inhibition of DDAH increases the intracellular concentration of ADMA enough to inhibit NOS activity, suggesting that DDAH contributes to the control of NO in vivo (*14*). The ADMA-DDAH pathway also contributes to several vascular diseases, including pulmonary hypertension (*15*–*17*).

We hypothesized that modulation of endogenous NOS inhibitors through changes in DDAH activity contributes to the pathogenesis of lung fibrosis. Here, we investigated the cellular expression of the two DDAH isoforms in the lungs of patients with IPF and in the lungs of mice with bleomycin-induced pulmonary fibrosis. We also explored whether DDAH is a direct target of profibrotic mediators and investigated the role of the ADMA-DDAH pathway in alveolar epithelial cell proliferation. We used the following five experimental approaches to evaluate the contribution of DDAH to pulmonary fibrosis in vivo: (i) treatment of bleomycin-challenged mice with the DDAH inhibitor L-291, (ii) treatment of bleomycin-challenged mice with ADMA, (iii) treatment of bleomycin-challenged mice with the iNOS inhibitor L-NIL, (iv) challenge of heterozygous DDAH1-overexpressing mice with bleomycin, and (v) challenge of iNOS-deficient mice with bleomycin followed by treatment with L-291 to explore whether DDAH exerts effects in addition to NO regulation.

[1]Max-Planck Institute for Heart and Lung Research, Bad Nauheim 61231, Germany. [2]University of Giessen Lung Centre, Giessen 35392, Germany. [3]Comprehensive Pneumology Center, University Hospital Grosshadern, Ludwig-Maximilians-University, and Helmholtz Zentrum München, Munich 81377, Germany. [4]Lungenfachklinik Waldhof-Elgershausen, Greifenstein 35753, Germany. [5]Medical Research Council, Clinical Sciences Centre, Imperial College London, Hammersmith Hospital, Du Cane Road, London W12 0NN, UK.
*To whom correspondence should be addressed: E-mail: ralph.schermuly@mpi-bn.mpg.de

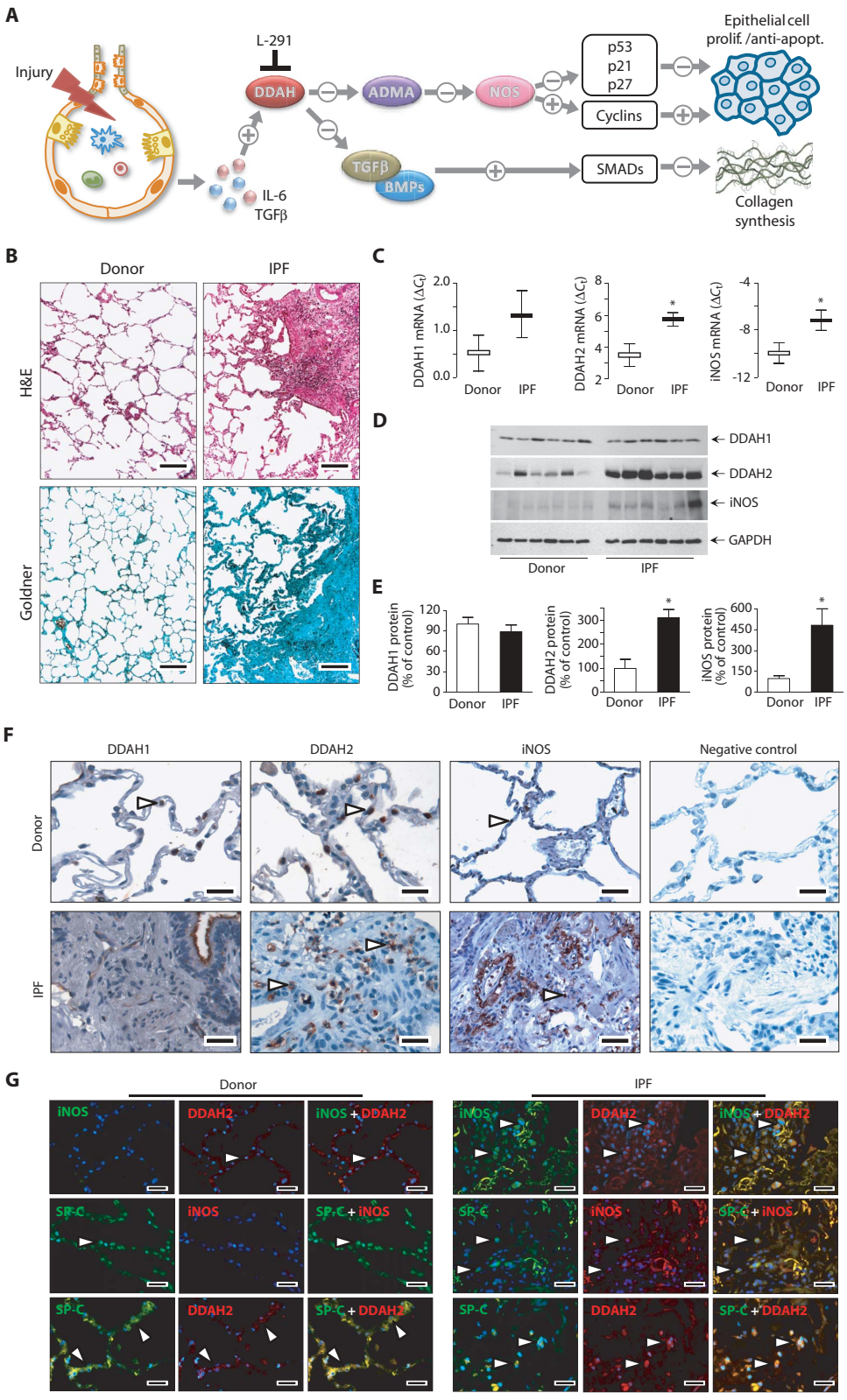

Fig. 1. Expression and localization of DDAH isoforms and iNOS in lungs from IPF patients and healthy donors. (**A**) Schematic diagram depicting the mechanisms whereby DDAH inhibition produces antiproliferative and antifibrotic effects. (**B**) Examples of serial H&E and Goldner's trichrome staining of lung sections (six per lung). (**C**) Quantitative RT-PCR analysis of DDAH1, DDAH2, and iNOS mRNA expression in lung tissues. The ΔC_t method was used to quantify relative changes. $n = 4$ lungs per group. (**D**) Western blot of DDAH1, DDAH2, iNOS, and a loading control [glyceraldehyde-3-phosphate dehydrogenase (GAPDH)] in lung homogenates. (**E**) Quantification of DDAH1, DDAH2, and iNOS protein normalized to GAPDH. Values are expressed as the percentage of expression found in donor tissue. $n = 6$ lungs per group. (**F**) Immunohistochemistry of DDAH1, DDAH2, and iNOS. In the negative control, the primary antibody was replaced with nonspecific immunoglobulin. (**G**) Double immunofluorescence staining of lung tissue with antibodies against DDAH2 (red), iNOS (green), and pro–SP-C (a marker specific for ATII cells, green). Merged images (yellow) of the same fields with 4′,6-diamidino-2-phenylindole (DAPI) counterstaining (blue) are also shown. Scale bars, 100 μm [(B), (F), and (G)]. Arrows, stained cells. $n = 6$ lungs per group in (B), (F), and (G). Data in (C) and (E) represent means ± SEM. *$P < 0.05$ versus healthy donor lungs.

RESULTS

Increased DDAH2 and iNOS expression in lungs from patients with IPF

We investigated the expression and localization of DDAH isoforms and iNOS in lungs from IPF patients undergoing lung transplantation. Hematoxylin-eosin (H&E) and Goldner's trichrome staining of sections from the explanted IPF lungs revealed the usual interstitial pneumonitis pattern, characterized by a lack of spatial homogeneity and profound collagen deposition, consistent with the diagnosis of IPF. Donor lungs showed regular lung architecture and no scarring (Fig. 1B). Expression of DDAH1 mRNA was similar in both the fibrotic and the donor lungs, whereas expression of DDAH2 and iNOS mRNA was significantly increased in IPF lungs compared to donor lungs (Fig. 1C). Protein levels of DDAH2 and iNOS were three times higher in IPF lungs than in donor lungs (Fig. 1, D and E).

Immunohistochemical staining showed that DDAH1 and DDAH2 were localized in the endothelium, inflammatory cells, fibroblasts, and alveolar and bronchiolar epithelium in donor lungs (Fig. 1F). In IPF

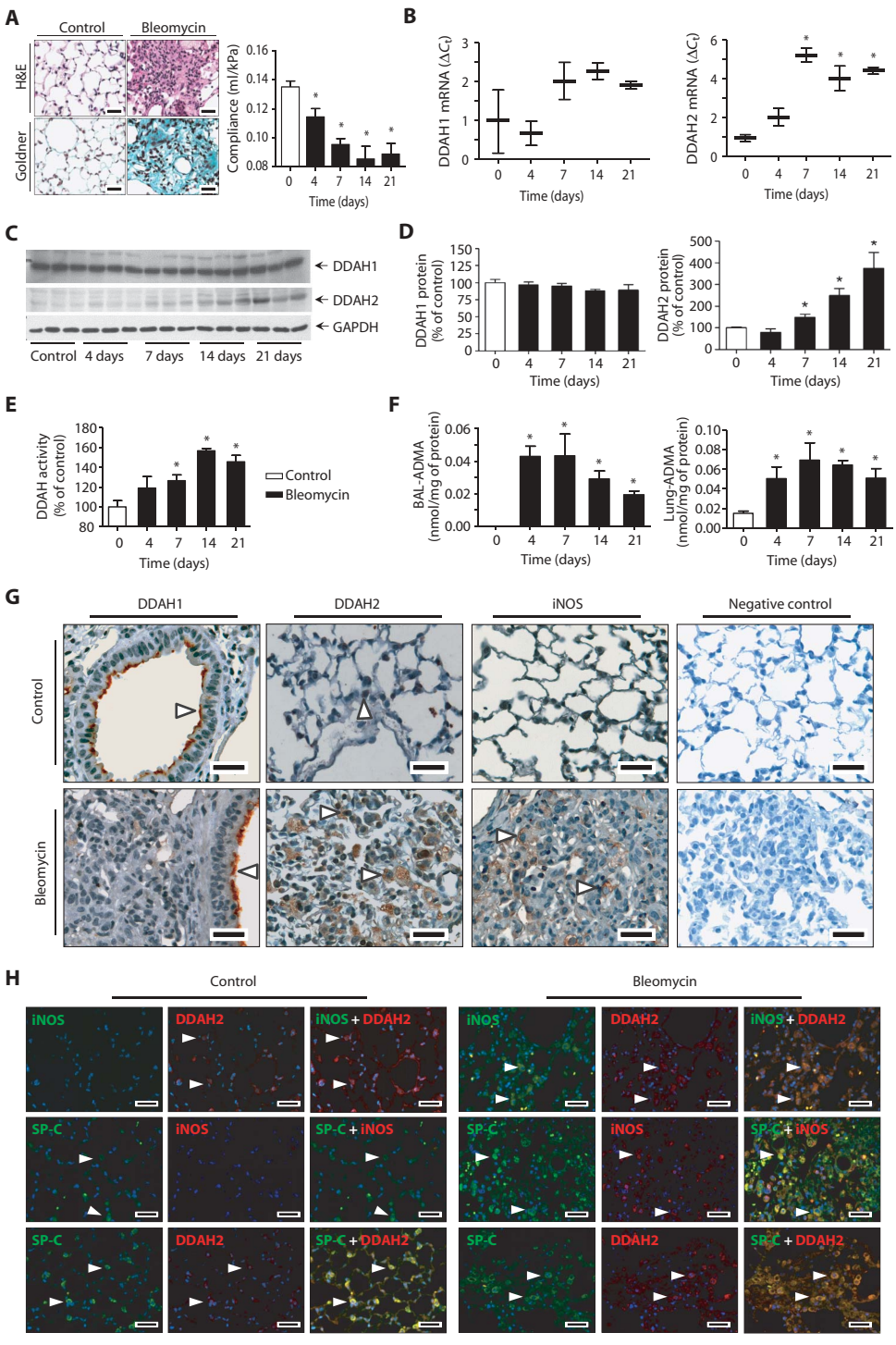

Fig. 2. Expression and localization of DDAH isoforms in lungs from control mice and mice with bleomycin-induced fibrosis. (**A**) Left: Serial H&E and Goldner's trichrome staining of lung sections. Right: Lung compliance measurements. (**B**) Quantitative RT-PCR analysis of DDAH1 and DDAH2 mRNA expression in lung tissues. The ΔC_t method was used to quantify relative changes. (**C**) Western blot of DDAH1, DDAH2, and a loading control (GAPDH) in lung homogenates. (**D**) Quantification of DDAH1 and DDAH2 protein normalized to GAPDH. Values are percentages of expression in tissue on day 0. (**E**) Total DDAH enzyme activity in lung homogenates. (**F**) ADMA levels in bronchoalveolar lavage (BAL) fluid and lung tissues. (**G**) Immunohistochemistry for DDAH1, DDAH2, and iNOS in lung sections. In the negative control, the primary antibody was replaced with a nonspecific immunoglobulin. (**H**) Double immunofluorescence staining of lung sections with antibodies against DDAH2 (red), iNOS (green), and pro–SP-C (a marker specific for ATII cells, green). Merged images (yellow) of the same fields with DAPI counterstaining (blue) also shown. Scale bars, 100 μm [(A), (G), and (H)]. Arrows, stained cells. $n = 6$ lungs per group. Data in (A) to (F) represent means ± SEM. *$P < 0.05$ versus day 0. $n = 3$ to 6 mice per group.

lungs, DDAH2 and iNOS were observed in close proximity to fibrotic scars, thickened septa, and fibroblast foci. IPF lungs also displayed colocalization of DDAH2 and iNOS (Fig. 1G). Costaining of DDAH2 and iNOS with pro–SP-C, a specific marker of alveolar type II (ATII) cells, revealed the presence of DDAH2 and iNOS in ATII cells lining the thickened septa (Fig. 1G).

Increased DDAH2 and iNOS expression and ADMA levels in mice with bleomycin-induced fibrosis

Compared to control mice, bleomycin-challenged mice displayed a severe loss of lung compliance, with collapse and obliteration of the alveolar spaces and extensive collagen deposition (Fig. 2A). Further analysis of DDAH1 and DDAH2 mRNA and protein in lung tissue sampled 4, 7, 14, and 21 days after the bleomycin challenge suggested that there is an induction of DDAH2 but no significant change in DDAH1 expression in response to bleomycin. DDAH2 mRNA, which was present at low levels in control mice, steadily increased from days 7 to 21 (Fig. 2, B to D). The increase in DDAH2 expression was mirrored by an increase in total DDAH enzyme activity, which peaked on days 7 to 21 (Fig. 2E). The ADMA content in both lung tissue and BAL fluid increased after the bleomycin challenge on days 4 to 7, but decreased thereafter (Fig. 2F).

Localization and colocalization of DDAH and NOS in mice with bleomycin-induced fibrosis

DDAH1 and DDAH2 immunoreactivity was detected in the endothelium, inflammatory cells, fibroblasts, airway epithelial cells, and alveolar epithelial cells of control lungs, and an increase was observed

in the alveolar epithelium of bleomycin-injured lungs (Fig. 2G). iNOS immunoreactivity was barely detectable in the lungs of control mice, but it was clearly present in the lungs of bleomycin-challenged mice (Fig. 2H). In addition, double immunostaining with pro–SP-C demonstrated that DDAH2 and iNOS were present in ATII cells and increased in the lungs of bleomycin-challenged mice (Fig. 2H). Similarly, DDAH2 mRNA expression was increased, and ADMA levels were decreased, in ATII cells isolated from bleomycin-challenged lungs (Fig. 3, A and B).

Regulation of DDAH by profibrotic mediators and the effects of DDAH inhibition on cell proliferation, apoptosis, and intracellular signaling

Because DDAH mRNA, protein, and enzyme levels were increased in bleomycin-induced fibrosis, we investigated the functional role of DDAH in ATII cells using L-291, a selective DDAH inhibitor. Serum stimulation induced a massive proliferation of ATII and MLE-12 cells, an alveolar epithelial cell line (Fig. 3, C and F), as measured by a thymidine incorporation assay. L-291 reduced this serum-induced proliferation in a dose-dependent manner, demonstrating that DDAH inhibition blocks DNA synthesis. L-291 also induced apoptosis of ATII cells in a dose-dependent manner (Fig. 3D). We further investigated the effects of L-291 on the expression of key control elements in the G_1-S phase transition in serum-stimulated ATII cells, including cyclins B, D, and E, as well as the cyclin-dependent kinase (CDK) inhibitors p21 and p27. L-291 did not alter the expression of cyclin B, but it increased p21 and p27 expression and decreased cyclin D and E expression after 24 hours (Fig. 3E). L-291 produced similar effects in MLE-12 cells (fig. S1).

We next investigated the mitogen-activated protein kinase (MAPK) pathway, which involves c-Jun N-terminal kinase (JNK), p38, and extracellular signal–regulated kinase (ERK) and is known to play a major role in proliferation. Exposure to L-291 or ADMA for 2 hours did not influence the phosphorylation status of ERK or JNK (fig. S1), indicating that the effect of DDAH-ADMA is independent of the MAPK pathway. Several reports have shown that p21 and p27 can be modulated by the p53 pathway (*18*, *19*). In addition, treatment of MLE-12 cells with L-291 increased p53 phosphorylation (Ser^6 and Ser^9; fig. S1). Together, these results suggest that L-291 suppresses alveolar epithelial cell proliferation through up-regulation of p21 and p27.

To assess the effect of the DDAH inhibitor on fibroblast growth, we isolated lung fibroblasts from mice, treated them with L-291, and analyzed them for proliferation and apoptosis. We found that L-291 produced a small decrease in fibroblast proliferation, but that it did not alter apoptosis (fig. S2).

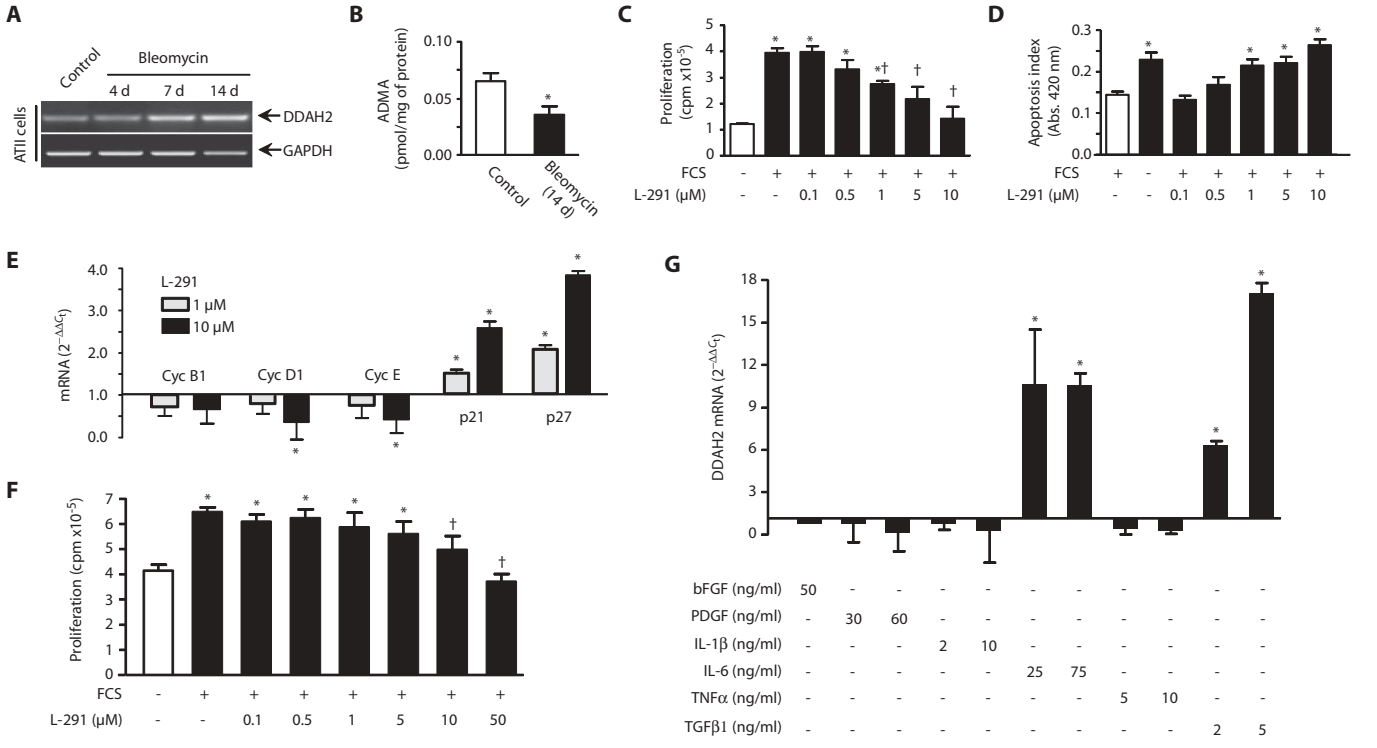

Fig. 3. DDAH regulates proliferation and apoptosis in ATII cells. (**A**) Expression of DDAH2 mRNA in primary ATII cells isolated from mice at 0 (control), 4, 7, and 14 days after bleomycin injury. (**B**) ADMA levels in primary ATII cells isolated from mice on day 0 (control) and at 14 days after bleomycin injury. *$P < 0.05$ versus day 0. $n = 4$ mice per group. (**C** to **E**) Primary ATII cells isolated from mice at 14 days after bleomycin injury were stimulated with fetal calf serum (FCS) and treated with L-291. Proliferation (C), apoptosis (D), and mRNA expression (E) of cyclins B, D, and E, p21, and p27. The $\Delta\Delta C_t$ method was used to quantify relative changes. $n = 3$ independent experiments. (**F**) Proliferation of MLE-12 cells stimulated with FCS and treated with L-291. (**G**) DDAH2 mRNA expression in serum-starved MLE-12 cells stimulated with basic fibroblast growth factor (bFGF), platelet-derived growth factor (PDGF), interleukin-1β (IL-1β), IL-6, tumor necrosis factor–α (TNFα), or transforming growth factor–β1 (TGFβ1). The $\Delta\Delta C_t$ method was used to quantify relative changes. *$P < 0.05$ versus serum-starved cells; †$P < 0.05$ versus serum-stimulated cells. $n = 3$ independent experiments.

Because DDAH was up-regulated in the late stages of fibrosis (days 7 to 21, Fig. 1), we investigated profibrotic mediators that might be involved. Quiescent MLE-12 cells were incubated with a variety of cytokines and growth factors (see Materials and Methods). Interleukin-6 (IL-6) and transforming growth factor–β1(TGFβ1) both caused a significant increase in DDAH2 mRNA expression (Fig. 3G).

Effect of DDAH2 gene silencing on cell proliferation, apoptosis, and intracellular signaling

To selectively study the function of DDAH2, we transfected MLE-12 cells with small interfering RNA (siRNA) for DDAH2. Reverse transcription–polymerase chain reaction (RT-PCR) and Western blot analysis revealed that transcription and expression of DDAH2, but not DDAH1, were knocked down 24 hours after transfection (Fig. 4, A and B). DDAH2 siRNA significantly decreased serum-induced proliferation and induced apoptosis in siRNA-transfected cells compared to control cells transfected with the cationic lipid-based transfection reagent Lipofectamine alone or control siRNA (Fig. 4, C and D). In addition, DDAH2 siRNA significantly decreased the expression of cyclin E and increased the expression of p21 and p27 (Fig. 4, E and F). These data suggest that DDAH2 plays an essential role in epithelial cell growth.

Effect of DDAH inhibition on bleomycin-induced fibrosis

To investigate the role of DDAH in experimental fibrosis, we treated bleomycin-challenged mice with saline, L-291 (10 mg/kg every third day for 21 days), or ADMA (30 mg/kg every third day for 21 days) (Fig. 5A). Bleomycin-challenged mice treated with L-291 exhibited a decrease in DDAH activity in lung lysates (Fig. 5B). Bleomycin-challenged mice that received saline displayed decreased lung compliance and weight loss over the 21-day treatment period (Fig. 5, C and D), whereas bleomycin-challenged mice treated with L-291 showed a significant improvement in lung function and an increase in body weight compared to saline-treated, bleomycin-challenged mice (Fig. 5, C and D). The effects of L-291 on body weight and lung function were more pronounced than those of ADMA (Fig. 5, C and D).

Histological analysis of bleomycin-treated mice revealed dense deposition of collagen, destruction of the normal tissue architecture, and a relative paucity of inflammatory cells, consistent with the final fibrotic stage of lung fibrosis (Fig. 5E). Treatment with L-291 reduced collagen deposition and tissue destruction (Fig. 5E). The extent of fibrosis, measured with the Ashcroft score, was significantly decreased by L-291 treatment, but not by ADMA treatment (Fig. 5F). The collagen content in lung lysates, quantified with the Sircol assay, was also significantly decreased by L-291 treatment, but not by ADMA treatment (Fig. 5G). Treatment with L-291 and ADMA each resulted in nearly normal levels of cell proliferation, as measured by the number of cells that were positive for proliferating cell nuclear antigen (PCNA; Fig. 5H). However, neither treatment reduced the number of inflammatory cells (neutrophils, macrophages, and lymphocytes) in the BAL fluid (Fig. 5I). These results suggest that both antifibrotic (ADMA-independent) and antiproliferative (ADMA-dependent) activities are involved in the inhibitory effects of L-291 on bleomycin-induced pulmonary fibrosis.

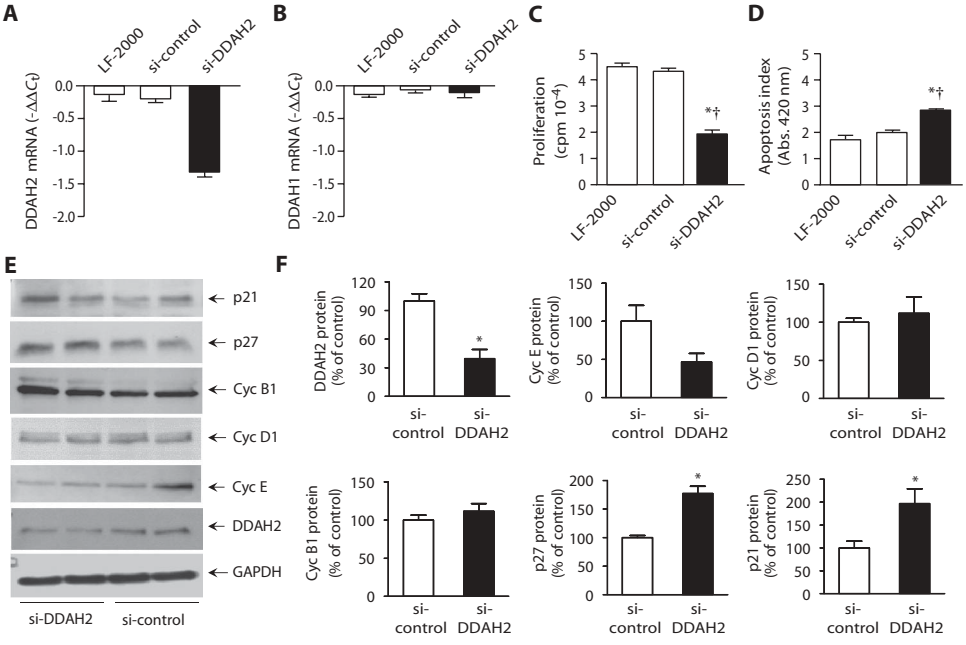

Fig. 4. Knockdown of DDAH2 by specific siRNA affects proliferation and apoptosis in ATII cells. MLE-12 cells were transiently transfected with Lipofectamine alone (LF-2000), 100 nM control siRNA (si-control), or 100 nM DDAH2 siRNA (si-DDAH2) for 24 hours. (**A** and **B**) mRNA expression of DDAH1 and DDAH2. The $\Delta\Delta C_t$ method was used to quantify relative changes. (**C** and **D**) Proliferation and apoptosis in transfected MLE-12 cells that were serum-starved for 24 hours and then stimulated with FCS. (**E** and **F**) Western blotting for DDAH2 and subsequent quantification of DDAH2, cyclins B1, D1, and E, p21, p27, and a loading control (GAPDH) in MLE-12 cells transfected with si-DDAH2 or si-control. Data in (A) to (D) and (F) represent means ± SEM. *$P < 0.05$ versus LF-2000 alone; †$P < 0.05$ versus si-control. $n = 4$ independent experiments.

Bleomycin-induced fibrosis in DDAH1-TG mice

To study the influence of DDAH overexpression in vivo, we challenged wild-type and transgenic mice that overexpress DDAH1 (DDAH1-TG) with bleomycin and examined them after 21 days. After the bleomycin challenge, the lungs of the wild-type mice displayed decreased lung compliance, dense collagen deposition, and parenchymal fibrosis. Further, these changes were substantially greater in the DDAH1-TG mice (Fig. 6, A and B). Quantification of the collagen content and histopathological changes in the lungs confirmed that there was indeed more collagen deposition in the DDAH1-TG mice (Fig. 6, C and D). In addition, the number of proliferating cells was also increased in the DDAH1-TG compared to wild-type mice (Fig. 6E). The number of inflammatory cells in the BAL fluid was similar in the two groups (Fig. 6F).

Effect of DDAH inhibition on residual pulmonary fibrosis in iNOS-deficient mice

We have demonstrated induction of iNOS expression, increased iNOS activity (*6*, *7*), and colocalization of iNOS with DDAH2 in ATII cells in bleomycin-challenged

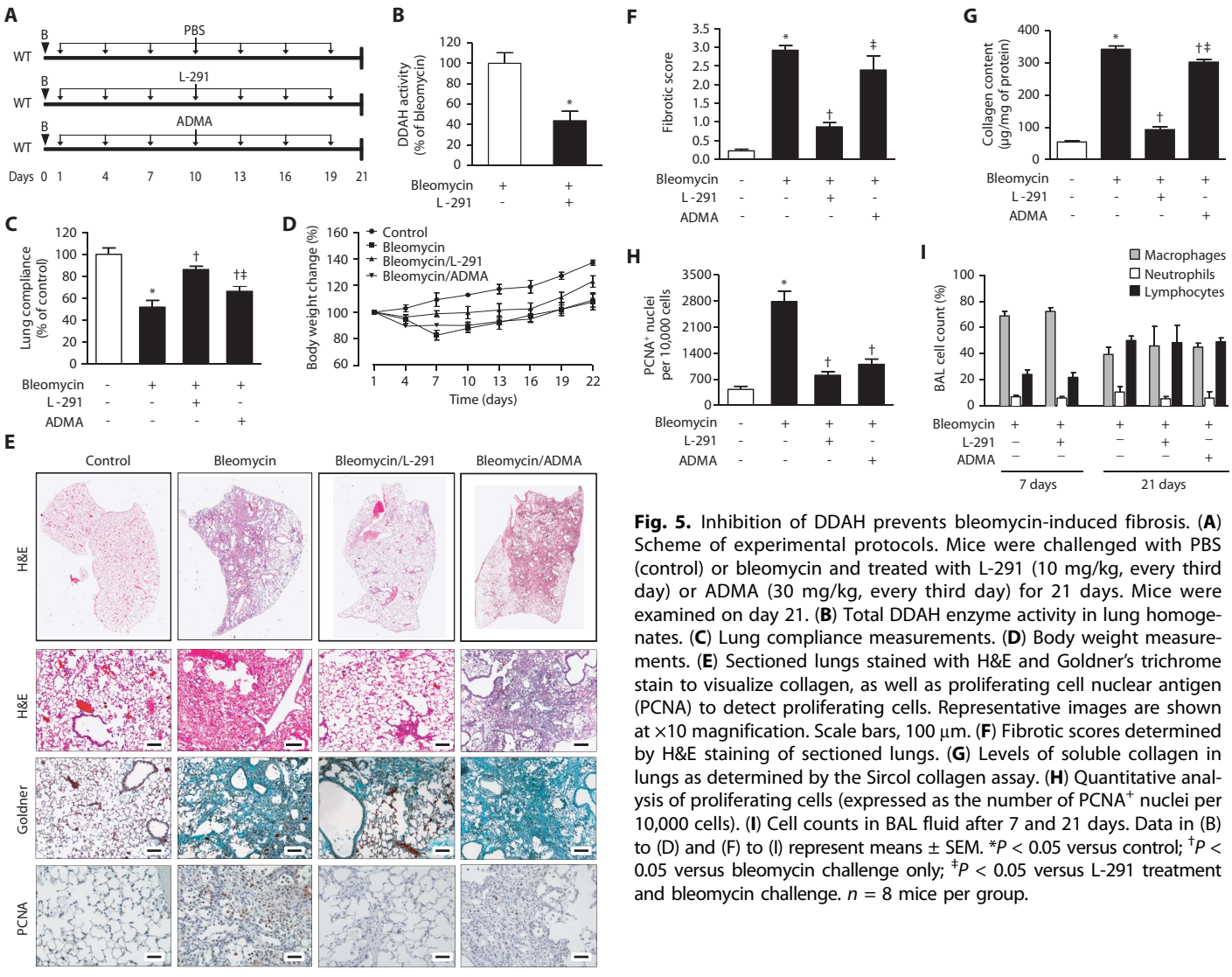

Fig. 5. Inhibition of DDAH prevents bleomycin-induced fibrosis. (**A**) Scheme of experimental protocols. Mice were challenged with PBS (control) or bleomycin and treated with L-291 (10 mg/kg, every third day) or ADMA (30 mg/kg, every third day) for 21 days. Mice were examined on day 21. (**B**) Total DDAH enzyme activity in lung homogenates. (**C**) Lung compliance measurements. (**D**) Body weight measurements. (**E**) Sectioned lungs stained with H&E and Goldner's trichrome stain to visualize collagen, as well as proliferating cell nuclear antigen (PCNA) to detect proliferating cells. Representative images are shown at ×10 magnification. Scale bars, 100 μm. (**F**) Fibrotic scores determined by H&E staining of sectioned lungs. (**G**) Levels of soluble collagen in lungs as determined by the Sircol collagen assay. (**H**) Quantitative analysis of proliferating cells (expressed as the number of $PCNA^+$ nuclei per 10,000 cells). (**I**) Cell counts in BAL fluid after 7 and 21 days. Data in (B) to (D) and (F) to (I) represent means ± SEM. $^*P < 0.05$ versus control; $^{\dagger}P < 0.05$ versus bleomycin challenge only; $^{\ddagger}P < 0.05$ versus L-291 treatment and bleomycin challenge. $n = 8$ mice per group.

mouse lungs. We wanted to determine whether the antifibrotic effects of DDAH inhibition were mediated via iNOS regulation. Bleomycin-challenged iNOS wild type (iNOS-WT) and iNOS-knockout (iNOS-KO) mice were treated with either saline or L-291, as described above (Fig. 7A). As expected, iNOS-KO mice were less affected by bleomycin treatment compared to iNOS-WT mice. Although lung compliance was similar, the bleomycin challenged iNOS-KO mice had an increased number of neutrophils, less fibrosis and lung collagen deposition, and reduced cell proliferation compared to wild-type mice (Fig. 7, B to G). However, treatment of iNOS-KO mice with L-291 increased both lung compliance and resistance to bleomycin-induced fibrosis (Fig. 7, B and C). The DDAH inhibitor caused significant reductions in alveolar destruction, fibrosis, and collagen deposition (Fig. 7, C to E) and produced a small decrease in cell proliferation (Fig. 7F). Nevertheless, the DDAH inhibitor decreased the number of neutrophils that were increased in iNOS-KO mice (Fig. 7G).

Notably, collagen production was significantly decreased in lung fibroblasts from wild-type and iNOS-KO mice challenged with bleomycin and treated with L-291 (Fig. 8A). This last finding suggests that DDAH inhibition may exert effects on the extracellular matrix (ECM) that are independent of iNOS inhibition.

To further delineate the role of iNOS, we treated bleomycin-challenged mice with either saline or L-NIL, a highly selective iNOS inhibitor (fig. S3A). Treatment with L-NIL caused a small improvement in the lung compliance of bleomycin-challenged mice and changed the cellular composition of BAL fluid but, ultimately, did not alter the degree of fibrosis (fig. S3, B and C).

Effects of DDAH inhibition on fibroblast collagen production

We further assessed the molecular mechanisms responsible for iNOS-independent regulation of the ECM (collagen) by DDAH inhibition. Administration of L-291, exogenous ADMA, and L-NIL had different effects on collagen production in TGFβ1-stimulated human lung fibroblasts. L-291 produced a dose-dependent inhibition of collagen production induced by TGFβ1 (fig. S4). Conversely, ADMA did not affect collagen production, and L-NIL partially decreased collagen production (Fig. 8B). Cotreatment with LDN193189, an inhibitor of bone morphogenetic protein (BMP), significantly reversed the effects of L-291,

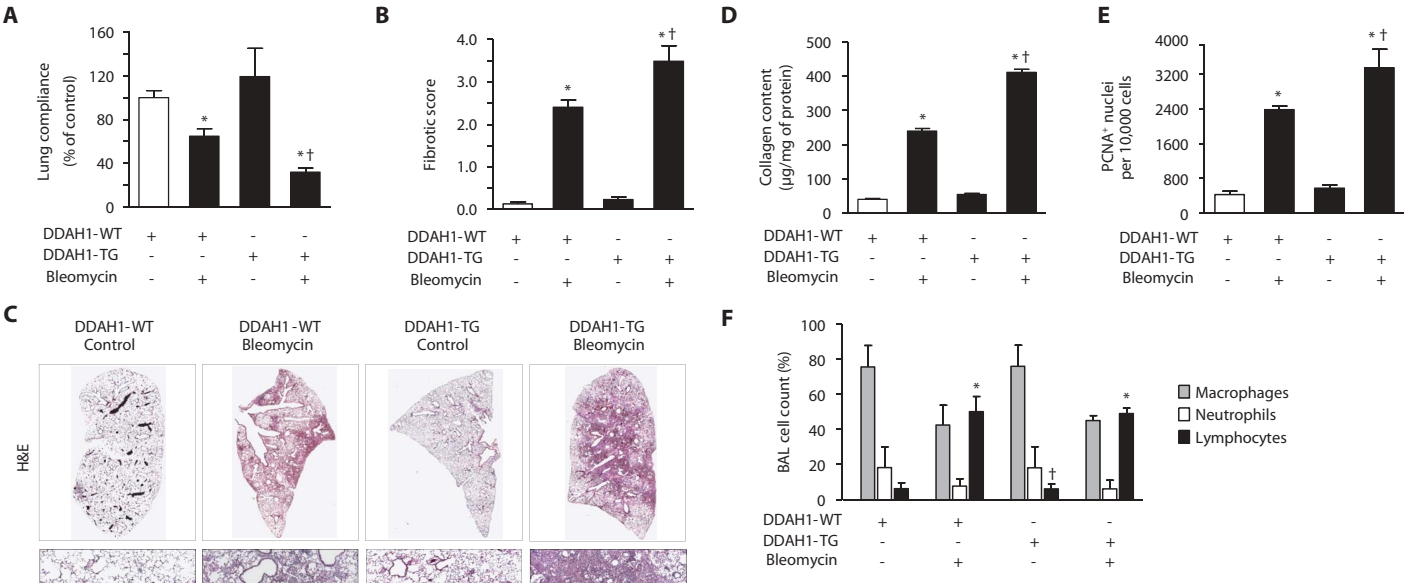

Fig. 6. Bleomycin-induced fibrosis is aggravated in DDAH1-TG mice. Wild-type (WT) and DDAH1-TG mice were challenged with saline (control) or bleomycin and examined on day 21. (**A**) Lung compliance measurements. (**B**) Fibrotic scores determined by H&E staining of sectioned lungs. (**C**) Sectioned lungs stained with H&E and Goldner's trichrome stain to visualize collagen, as well as PCNA to detect proliferating cells. Representative images are shown at ×10 magnification. Scale bars, 100 μm. (**D**) Levels of soluble collagen in lungs as determined by the Sircol collagen assay. (**E**) Quantitative analysis of proliferating cells (expressed as the number of $PCNA^+$ nuclei per 10,000 cells). (**F**) Cell counts in BAL fluid on day 21. Data in (A), (B), and (D) to (F) represent means ± SEM. $^*P < 0.05$ versus control; $^\dagger P < 0.05$ versus bleomycin treatment. $n = 8$ mice per group.

but not of ADMA or L-NIL, on collagen production induced by TGFβ1 (Fig. 8B).

We next investigated the role of BMP receptors and their downstream signaling molecules in the L-291–mediated inhibition of collagen production by TGFβ1-stimulated human lung fibroblasts. Real-time RT-PCR indicated that L-291 produced an increase in the expression of mRNA for helix-loop-helix proteins, particularly ID1, ID2, and ID3, which are direct targets of the BMP/SMAD signaling pathway. L-291 treatment also increased the mRNA expression of Smad1, Smad5, Smad6, and follistatin, a strong antagonist of activin A (Fig. 8C). However, L-291 treatment did not alter the expression of BMP ligands, BMP receptors, or endogenous inhibitors of BMP (fig. S5). The fact that L-291 treatment increased the expression of BMP target genes suggests that BMP signaling was activated. Although baseline Smad1/5/8 phosphorylation was not altered in fibroblasts treated with L-291 (Fig. 8, D and E), a significant increase was seen in lungs from bleomycin-challenged mice treated with L-291 (Fig. 8, F and G). To confirm that BMP signaling was activated by L-291 treatment, we transfected NIH 3T3 fibroblasts with a BMP-responsive promoter located upstream of a firefly luciferase gene on the pID120 reporter plasmid. Administration of a BMP ligand increased relative luciferase activity in the transfected fibroblasts, and L-291 addition further enhanced relative luciferase activity (Fig. 8H). These results suggest that L-291 accelerates BMP signaling by enhancing the transcriptional activity of BMP-responsive elements.

DISCUSSION

We have demonstrated increased expression and activity of DDAH in ATII cells, both in a murine model of pulmonary fibrosis and in the lungs of patients with IPF. In addition, using freshly isolated ATII and mouse transformed lung epithelial (MLE-12) cells, we identified TGFβ1 and IL-6 as inducers of DDAH expression. Both the pharmacological inhibition of DDAH by L-291 and the loss of function of DDAH caused by DDAH2-selective siRNA attenuated alveolar epithelial cell proliferation and apoptosis in vitro, showing the role of DDAH in these processes. These effects appeared to be mediated by the ADMA-p53-p21 signaling axis. The role of DDAH signaling in pulmonary fibrosis was confirmed in vivo; treatment of bleomycin-challenged mice with a selective DDAH inhibitor prevented bleomycin-induced pulmonary fibrosis, reduced collagen deposition and overall cellularity, and restored lung function to near-normal levels, but it did not affect inflammatory cell infiltration, with the exception that it reduced neutrophils in iNOS-KO but not wild-type mice. Bleomycin-induced fibrosis was more severe in DDAH1-overexpressing mice. Furthermore, ADMA and iNOS inhibitor treatment of bleomycin-challenged mice, as well as DDAH inhibitor treatment of iNOS-deficient, bleomycin-challenged mice, demonstrated that in bleomycin-induced fibrosis, iNOS inhibition decreased fibrosis and that an even stronger reduction was observed after simultaneous inhibition of DDAH. We conclude that DDAH inhibition reduces fibroblast-induced collagen production in an ADMA-independent

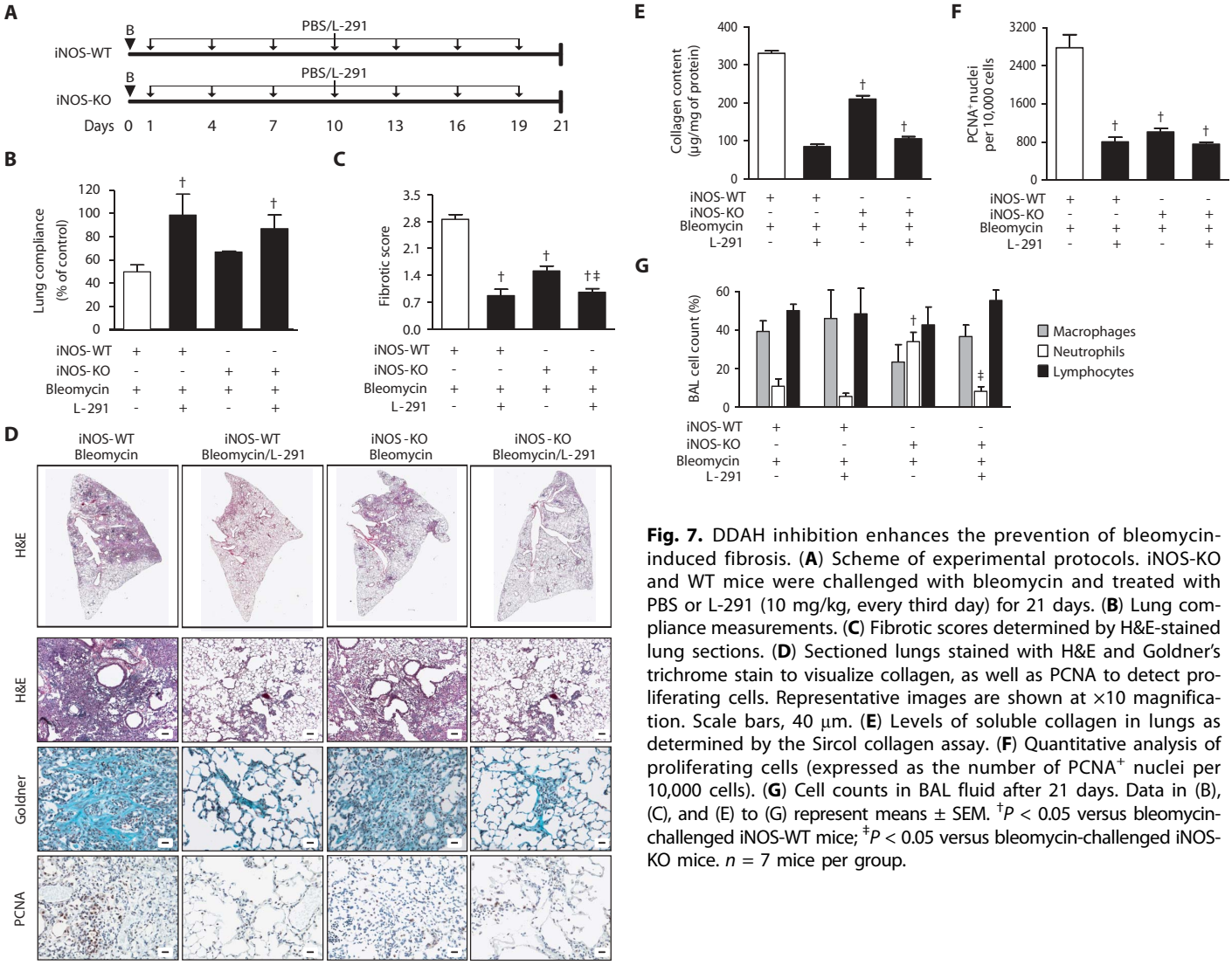

Fig. 7. DDAH inhibition enhances the prevention of bleomycin-induced fibrosis. (**A**) Scheme of experimental protocols. iNOS-KO and WT mice were challenged with bleomycin and treated with PBS or L-291 (10 mg/kg, every third day) for 21 days. (**B**) Lung compliance measurements. (**C**) Fibrotic scores determined by H&E-stained lung sections. (**D**) Sectioned lungs stained with H&E and Goldner's trichrome stain to visualize collagen, as well as PCNA to detect proliferating cells. Representative images are shown at ×10 magnification. Scale bars, 40 μm. (**E**) Levels of soluble collagen in lungs as determined by the Sircol collagen assay. (**F**) Quantitative analysis of proliferating cells (expressed as the number of $PCNA^+$ nuclei per 10,000 cells). (**G**) Cell counts in BAL fluid after 21 days. Data in (B), (C), and (E) to (G) represent means ± SEM. $^{\dagger}P < 0.05$ versus bleomycin-challenged iNOS-WT mice; $^{\ddagger}P < 0.05$ versus bleomycin-challenged iNOS-KO mice. $n = 7$ mice per group.

manner and reduces abnormal epithelial proliferation in an ADMA-dependent manner. Thus, DDAH inhibition may offer a therapeutic approach for attenuation of pulmonary fibrosis.

Currently, there are no effective treatments for IPF. Past efforts have focused on treating the underlying inflammation with potent and prolonged anti-inflammatory therapy in combination with immune modulatory drugs, but this approach is ineffective (*20*). New proposed therapeutic approaches that have been tested in clinical trials include the following: interferon-γ (*21*); pirfenidone, which targets the TGFβ pathway (*22*); bosentan, which targets the endothelin pathway (*23*); and *N*-acetylcysteine, which reduces oxidative stress (*24*). Of these, only *N*-acetylcysteine produced a significant improvement in the primary study endpoint in IPF patients enrolled in the IFIGENIA trial (*24*), although the trial was associated with a high dropout rate.

In several studies, ADMA has been identified as a risk factor for endothelial dysfunction–associated diseases like hypercholesterolemia, hyperhomocysteinemia, diabetes mellitus, and pulmonary hypertension in humans (*25*, *26*). Further, plasma concentrations of ADMA are increased and expression of DDAH is decreased both in patients with pulmonary hypertension and in an animal model of this disease (*15*). Deletion or inhibition of DDAH increases right ventricular pressures and induces structural changes in the pulmonary vasculature (*16*). To date, however, there has been no evidence for the presence of DDAH in cell types other than endothelial and immune cells.

We have shown that DDAH is expressed in the ATII cells of healthy lungs, and that this expression is markedly increased in the lungs of IPF patients and mice with bleomycin-induced fibrosis. These findings are consistent with the hypothesis that DDAH may be an important regulator of ATII cell biology. Furthermore, we demonstrated that DDAH2 and iNOS colocalize in the same cells and have close spatial relationships to thickened septa and scar tissue, as would be expected if DDAH regulates iNOS in the fibrotic lung. We demonstrated the regulation of DDAH in lungs both from IPF patients and from mice with bleomycin-induced fibrosis, which we found particularly interesting because the initial triggers for the development of fibrosis are clearly distinct (idiopathic in humans and inflammation

in the mouse model) (*3*). This finding suggests that the NO response in pulmonary fibrosis is not necessarily triggered by a unique mechanism but, rather, may represent a more general response to wound repair.

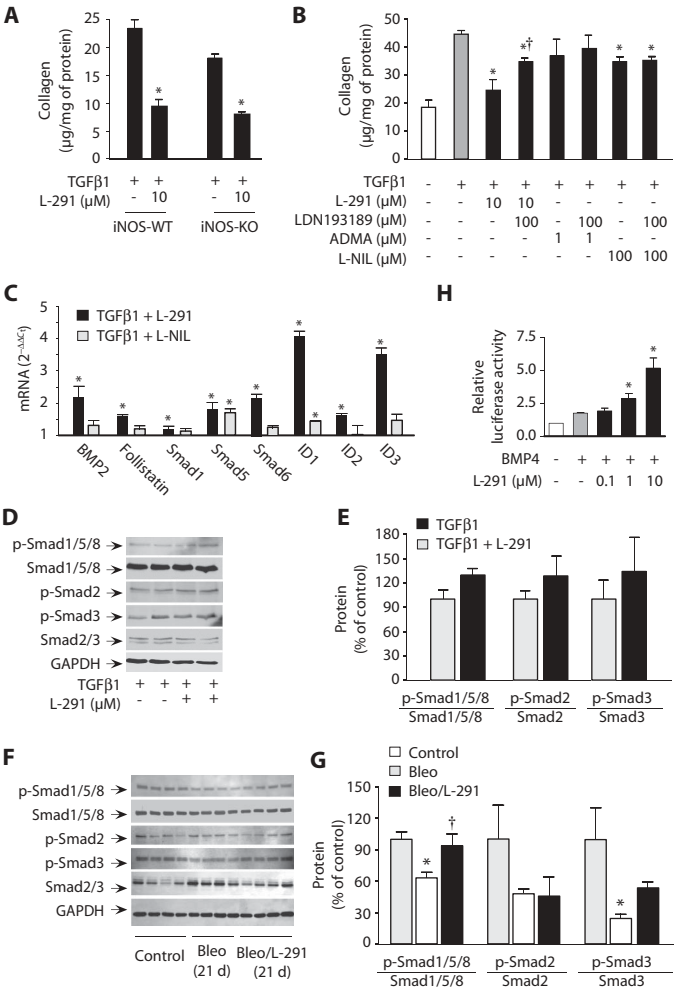

Fig. 8. DDAH inhibition attenuates collagen production in fibroblasts by means of iNOS-independent and BMP/SMAD pathways. (**A**) Fibroblasts isolated from bleomycin-challenged iNOS-WT and iNOS-KO mice lung tissues were stimulated with TGFβ1 (5 ng/ml) in the presence of L-291. (**B**) Human lung fibroblasts were stimulated with TGFβ1 (5 ng/ml) in the presence of L-291, ADMA, L-NIL, or LDN193189. Collagen content was determined by the Sircol collagen assay. (**C**) mRNA expression of BMP2, follistatin, Smad1, Smad5, Smad6, ID1, ID2, and ID3. The $\Delta\Delta C_t$ method was used to quantify relative changes. *$P < 0.05$ versus TGFβ1 treatment; †$P < 0.05$ versus L-291 treatment. (**D**) Western blot of phosphorylated Smad1/5/8 (p-Smad1/5/8), Smad1/5/8, p-Smad2, p-Smad3, Smad2/3, and a loading control (GAPDH). (**E**) Quantification of p-SMAD normalized to total SMAD. (**F**) Lungs from control or bleomycin-challenged mice treated with PBS or L-291 were used for Western blotting using antibodies against p-Smad1/5/8, Smad1/5/8, p-Smad2, p-Smad3, Smad2/3, and a loading control (GAPDH). (**G**) Quantification of p-SMAD normalized to total SMAD. (**H**) NIH 3T3 cells were transfected with BMP-responsive reporter pID120, followed by stimulation with BMP4 (20 ng/ml) in the presence of L-291 (0.1, 1, and 10 μM), and luciferase activity was measured. $n = 3$ independent experiments. Data in (A) to (C), (E), (G), and (H) represent means ± SEM. *$P < 0.05$ versus control; †$P < 0.05$ versus bleomycin challenge. $n = 4$ mice per group.

Indeed, ongoing experimental and clinical wound-healing studies suggest that NO is a critical mediator of wound repair (*27*). For example, in diabetic patients with foot ulcers, decreased levels of NO and increased levels of ADMA in wound fluid are indicators of impaired wound healing (*28*). In contrast, induction of iNOS in the fibrotic plaques of patients with Peyronie's disease protects against fibrosis and abnormal wound healing (*29*). Some studies suggest that pulmonary fibrosis results from abnormal alveolar wound repair and remodeling in the lung, so it is reasonable that NO may contribute to the pathogenesis of pulmonary fibrosis (*30*). There are strong similarities between animal models of pulmonary fibrosis (bleomycin-induced lung injury) and general wound models with respect to inflammatory responses, coagulation cascades, and other downstream responses (*31*). Similarly, we observed that the DDAH-NO system is altered in both experimental and clinical pulmonary fibrosis.

Enhanced expression of DDAH in pulmonary fibrosis and its role in the regulation of NO homeostasis may be explained by several mechanisms. DDAH expression and activity are enhanced by cytokines (*32*). We found that TGFβ1 up-regulated DDAH2 expression in a time-dependent manner in vitro. TGFβ1, a well-described profibrotic cytokine, is up-regulated at sites of fibrogenesis and is involved in a variety of cellular responses that contribute to fibrosis (*33*). Transcriptional modulation of DDAH2 is also mediated via IL-6, a well-known fibrogenic cytokine (*34*). Induction of DDAH2 by profibrotic mediators in vitro and overexpression of DDAH2 in hyperplastic ATII cells in vivo suggest that DDAH may regulate the epithelial cell damage, aberrant tissue regeneration, epithelial-mesenchymal transition, and fibroproliferation that occur in pulmonary fibrosis.

Earlier studies delineating the functions of DDAH primarily focus on endothelial dysfunction (*26*), tissue regeneration (*17*), and angiogenesis (*35*). We found that inhibition of DDAH markedly inhibited proliferation of, and induced apoptosis in, ATII cells. These functional changes are characteristic of reduced levels of endogenous NO, and the same results were observed when ATII cells were treated with ADMA. A large body of evidence indicates that telomerase and p38 are associated with ADMA-induced endothelial cell apoptosis (*12*). In our studies, treatment of epithelial cells with a selective DDAH inhibitor, DDAH2-specific siRNA, or ADMA increased the phosphorylation of p53, p21, and p27, but did not have any effect on MAPK activation. In addition, bleomycin-challenged mice treated with the DDAH inhibitor displayed a reduction in lung cellularity, which may be a result of reduced proliferation and/or increased cell death of hyperplastic ATII cells. Furthermore, the DDAH inhibitor prevented bleomycin-induced pulmonary fibrosis in this mouse model.

It is currently unclear whether decreased epithelial proliferation and/or increased epithelial apoptosis attenuate or enhance lung fibrosis. Ultrastructural studies have revealed the existence of proliferative ATII cells immediately adjacent to injured epithelial cells in IPF (*36*, *37*), suggesting that apoptosis and proliferation of epithelial cells and hyperplasia occur simultaneously during the fibrotic process. In experimental models of lung fibrosis, epithelial cell damage is caused by bleomycin (*38*), and epithelial cell apoptosis precedes the onset of tissue fibrosis and alveolar remodeling in TGFβ1 transgenic mice (*39*, *40*). By contrast, studies have shown that ATII cells isolated from fibrotic lungs 14 days after bleomycin instillation exhibit an increased proliferative capacity and enhanced gene expression of proliferative mediators (*41*). Similarly, Degryse *et al.* demonstrated that lungs from mice repeatedly treated with bleomycin display marked fibrosis with prominent ATII

cell hyperplasia, which are features reminiscent of usual interstitial pneumonia (*42*).

It is not known whether hyperplastic epithelial cells are beneficial (for instance, by providing a source for alveolar epithelial cell renewal) or harmful (by acting as producers of profibrotic signals). Moreover, recent observations suggest that these activated cells undergo an epithelial-to-mesenchymal transition, which can significantly contribute to the pool of expanded fibroblasts after lung injury (*43*, *44*). Because DDAH2 expression is increased in hyperplastic epithelial cells, and treatment with a DDAH inhibitor decreased proliferation and increased apoptosis of ATII cells isolated from bleomycin-treated lungs in vitro and inhibited cell proliferation in vivo, we surmise that L-291 blocks ATII cell hyperplasia and activation, ultimately leading to attenuation of bleomycin-induced pulmonary fibrosis.

A key finding of this study is that DDAH inhibition decreased collagen deposition, decreased the overall lung cellularity, and prevented pulmonary fibrosis, with near normalization of lung function. DDAH inhibition had no effect on inflammatory cell influx (with the exception of its effects on neutrophils in iNOS-KO mice), but it did modulate key fibrotic signaling cascades, leading us to believe that DDAH inhibition may provide a new therapeutic approach for patients with IPF. The contribution of DDAH to the fibrotic process was further confirmed by studies of DDAH1-overexpressing mice, which displayed markedly more severe pulmonary fibrosis than wild-type controls. Although DDAH2 is the predominant DDAH isoform that was overexpressed in fibrotic lungs, we used DDAH1-overexpressing mice in the present study. Mice that overexpress DDAH1, similar to DDAH2-overexpressing mice, displayed a reduction in plasma ADMA levels and a concomitant increase in tissue levels of NO (*14*, *45*). These findings, as well as nonavailability of DDAH2-overexpressing mice, led us to use DDAH1-overexpressing mice. However, recent studies with DDAH1- and DDAH2-selective siRNAs revealed potentially different regulatory roles of DDAH1 versus DDAH2 (*46*). Hence, further studies with DDAH2 transgenic mice are required to further define the specific role of DDAH2 in fibrotic processes in vivo.

In contrast, exogenous ADMA decreased proliferation and induced apoptosis, but only partially affected lung compliance and did not influence collagen deposition. Therefore, the effect of DDAH on collagen deposition may be not mediated by its inhibition of ADMA. Consistent with this interpretation, we found that the DDAH inhibitor and exogenous ADMA exerted differential effects on ECM production in activated human lung fibroblasts, whereas only the DDAH inhibitor decreased collagen production.

In agreement with previous studies (*47*), our iNOS-KO mice showed less collagen deposition and less proliferation in response to bleomycin treatment, suggesting a role for iNOS in this model. However, treatment with the DDAH inhibitor L-291 markedly decreased neutrophils in iNOS-KO mice, but not in wild-type mice. Neutrophil alterations are implicated in lung fibrosis (*48*), and recently, a possible role for IL-17–dependent pathogenic mechanisms has been discussed (*49*). Thus, the decrease in fibrosis by L-291 in iNOS-KO mice could be explained by the reduction in neutrophils in those mice. Treatment of these mice with the DDAH inhibitor L-291 caused a stronger reduction of collagen content in vivo and in vitro than in bleomycin treated iNOS-KO mice, implying that inhibition of DDAH has effects on the ECM that are independent of iNOS inhibition.

Because L-291 inhibits DDAH (*16*) and cross-reactivity with other signaling molecules has not been reported, our findings may be explained by regulation of other NOS isoforms or by NO-independent effects of DDAH. Because compensatory regulation of other NOS isoforms has been reported in endothelial NOS (eNOS)–KO or iNOS-KO mice (*50*), we tested the effects of L-NIL, a selective iNOS inhibitor. L-NIL treatment had minimal effects on bleomycin-induced pulmonary fibrosis. A recent report suggests that DDAH up-regulates the expression of vascular endothelial growth factor (VEGF) through Sp1-dependent and NO/NOS-independent promoter activation (*51*). We observed iNOS-independent activation of the BMP/SMAD signaling pathway associated with suppression of the ECM. This regulation is of potential importance because recent studies suggest that regulation of BMP signaling activity may represent a beneficial treatment strategy for pulmonary fibrosis (*52*).

In conclusion, DDAH plays an important pathophysiological role in pulmonary fibrosis. We present evidence that DDAH inhibition suppresses experimental pulmonary fibrosis via ADMA-dependent regulation of cell growth and ADMA-independent regulation of the ECM. Further evaluation of this pathway in human fibrosis may provide a therapeutic approach for the treatment of this insidious and irreversible disease.

MATERIALS AND METHODS

All human and animal experiments were approved by the local ethics committees according to the guidelines of the German Physiological Society.

Patients, clinical data, and tissue handling

Twelve patients [age, 57.4 ± 4.1 (mean ± SEM) years; seven male, five female] diagnosed with IPF according to the international consensus statement (*53*) were included in this study. BAL fluid was obtained from six patients, and lung tissue was obtained from the other six patients. Control tissue was obtained from six donor lungs that could not be transplanted because of incompatibility between the donor and the recipient, and plasma samples were obtained from 10 healthy volunteers with normal lung function. See the Supplementary Material for details. Lung tissue specimens for mRNA and protein extraction were immediately frozen in liquid nitrogen after explantation. Lung tissue specimens for immunohistochemical or immunofluorescence staining were directly transferred into 4% buffered paraformaldehyde.

Bleomycin-induced lung fibrosis

C57BL/6 mice (6 to 8 weeks old, 20 to 25 g) were intratracheally injected with bleomycin (3 U/kg; Sigma) in 80 μl of 0.9% saline. Control mice were given 80 μl of 0.9% saline intratracheally. DDAH1-TG mice, iNOS-KO mice, and their corresponding wild-type littermates (Jackson Laboratories) were challenged with bleomycin in the same way.

The day after the bleomycin challenge, the bleomycin-treated mice were randomly assigned to treatment with L-291 (*16*) [10 mg/kg in phosphate-buffered saline (PBS)], ADMA (30 mg/kg in PBS), L-NIL (10 mg/kg in PBS), or an equivalent volume of PBS, administered by oral gavage every third day for 21 days. Body weight was measured on each day of treatment, and lung compliance was measured on days 4, 7, 14, and 21 after bleomycin administration. See the Supplementary Material for additional details.

Histopathological examination and quantification of fibrosis

Murine lung samples were fixed in formalin and embedded in paraffin. Sections were stained with H&E to visualize morphology and Goldner's

trichrome stain to determine the extent and local sites of collagen deposition. For histological assessment, slides from all four lobes were scanned with a light microscope (Leica) at ×100 magnification to collect 50 to 100 images per lobe (that is, up to 300 images per animal). The degree of fibrosis in each image was scored in a blinded fashion with the Ashcroft fibrosis scoring system (*54*) with a slight modification (range, 0 for normal tissue to 5 for maximal fibrotic pathology).

Immunohistochemical and immunofluorescence staining

Paraffin-embedded lung tissue sections (3 μm thick) were deparaffinized in xylene and rehydrated in a graded ethanol series to PBS (pH 7.2). Antigen retrieval was performed by pressure cooking in citrate buffer (pH 6.0) for 15 min. Immunohistochemical staining was performed with antibodies against PCNA (to assess cellular proliferation in vivo), iNOS, pro–SP-C, DDAH1, and DDAH2, in combination with an avidin-biotin-peroxidase kit (Zymed Laboratories Inc.), as described (*55*). The signal was developed by incubating with AEC (3-amino-9-ethylcarbazole) substrate. Sections were counterstained with hematoxylin and covered with a coverslip. To evaluate the spatial localization of DDAH2 and iNOS, we performed double immunofluorescence staining with antibodies against DDAH2, iNOS, and pro–SP-C.

Bronchoalveolar lavage

Lungs were lavaged with three sequential 0.5-ml volumes of PBS 7 and 21 days after administration of bleomycin or saline. BAL fluid was pooled and centrifuged, and the cell pellet was resuspended in PBS. Cells were counted with a hemocytometer, and a differential cell count was performed after centrifugation in a Cytospin 3 centrifuge (Shandon Scientific Ltd.) with May Grunwald/Giemsa staining and standard light microscopy techniques.

Quantitative PCR

Quantitative PCR was performed to evaluate the relative mRNA expression changes of DDAH and NOS isoforms in cells and lung tissue. See the Supplementary Material for details.

Western blotting

Details of the Western blotting and the antibodies that were used are described in the Supplementary Material.

DDAH activity

DDAH activity was indirectly measured with a colorimetric assay to observe the formation of L-citrulline from ADMA in tissue homogenates (*15*). As a negative control, tissue homogenates were boiled for 10 min to inactivate the enzyme. Background values were subtracted from experimental values. One unit of enzyme was defined as the amount of enzyme that catalyzed the formation of 1 μmol L-citrulline per minute at 37°C.

Quantification of ADMA

ADMA was quantified from tissue extracts and BAL fluid as described in the Supplementary Material.

Cell lines

Mouse NIH 3T3 fibroblasts and A549 and MLE-12 cells were obtained from the American Type Culture Collection. NIH 3T3 and A549 cells were cultured in Dulbecco's modified Eagle's medium (DMEM) (Invitrogen) supplemented with 10% fetal calf serum (FCS; HyClone) and 1% penicillin/streptomycin in a humidified 5% CO_2 incubator at 37°C. MLE-12 cells were cultured in DMEM/F12 medium supplemented with 10% FCS and 1% penicillin/streptomycin in a humidified 5% CO_2 incubator at 37°C.

Stimulation of cell lines

MLE-12 cells were serum-starved for 24 hours and incubated with basic fibroblast growth factor (bFGF; 50 ng/ml), platelet-derived growth factor (PDGF; 30 and 60 ng/ml), IL-1β (2 and 10 ng/ml), IL-6 (25 and 75 ng/ml), tumor necrosis factor–α (TNFα; 5 and 10 ng/ml), or TGFβ1 (2 and 5 ng/ml) for 24 hours to quantify relative changes in mRNA expression by quantitative PCR.

siRNA experiments

Endogenous DDAH2 expression in MLE-12 cells was knocked down with a DDAH2 siRNA target sequence (sense, 5′-GGCAGUGUCUCGAGAACUU-3′; antisense, 5′-AAGUUCUCGAGACACUGCC-3′; Eurogentec, 100 nM). A negative control siRNA sequence (Eurogentec, 100 nM) was used as a specificity control. MLE-12 cells were transiently transfected with the cationic lipid-based transfection reagent Lipofectamine (Invitrogen) according to the manufacturer's recommendations. The transfection efficiency was assessed by real-time RT-PCR with DDAH1 and DDAH2 primers and by Western blotting to detect DDAH2 with an anti-DDAH2 antibody.

Reporter gene assays

NIH 3T3 cells were seeded in 24-well plates and transiently transfected with pID120 (which contains a BMP-responsive promoter placed immediately upstream of a firefly luciferase gene) (*56*), or with pGL3-basic (which contains a luciferase gene without a promoter) or pGL3-control (which contains a constitutively expressed luciferase gene) as negative and positive controls, respectively. All plasmids were purchased from Promega, and transfections were performed with Lipofectamine according to the manufacturer's recommendations. Cells were stimulated with BMP4 (20 ng/ml) in the presence or absence of L-291 for 12 hours. Cells were lysed and processed for determination of firefly luciferase activity as instructed by the manufacturer. Values were normalized for the transcriptional activity of the pGL3-control vector.

Isolation and culture of ATII cells

ATII cells were isolated and cultured as described in the Supplementary Material.

Isolation and culture of human and mouse interstitial fibroblasts

Primary lung fibroblasts were isolated and cultured from human and murine lungs. Methodological details are described in the Supplementary Material.

Collagen assays

To study the influence of various factors on TGFβ1-induced collagen production, we incubated quiescent fibroblasts with TGFβ1 (5 ng/ml) for 24 hours in the presence or absence of the DDAH inhibitor L-291 (0.1, 1, and 10 μM), ADMA (1 μM), the iNOS inhibitor L-NIL (100 μM), or the BMP inhibitor LDN193189 (100 μM). The level of acid-soluble collagen in these samples and in lung tissue was determined with a Sircol collagen assay (Biocolor Ltd.) according to the manufacturer's instructions.

Proliferation and apoptosis assays

The effects of L-291 and ADMA on the proliferation and apoptosis of ATII and MLE-12 cells and fibroblasts were assessed as described in the Supplementary Material.

Data analysis

All data are presented as means ± SEM. Differences between groups were assessed by one-way analysis of variance (ANOVA) and Student-Newman-Keuls post hoc tests for multiple comparisons. A P value of <0.05 was considered significant.

SUPPLEMENTARY MATERIAL

www.sciencetranslationalmedicine.org/cgi/content/full/3/87/87ra53/DC1
Materials and Methods
Fig. S1. DDAH inhibition regulates proliferation and apoptosis in MLE-12 cells, an ATII cell line.
Fig. S2. DDAH inhibition regulation of fibroblast proliferation or apoptosis.
Fig. S3. Pharmacological inhibition of iNOS in bleomycin-induced fibrosis.
Fig. S4. DDAH inhibition attenuates collagen production in fibroblasts in a dose-dependent manner.
Fig. S5. DDAH inhibition regulates molecules in the BMP/SMAD signaling pathway.
References

REFERENCES AND NOTES

1. M. Selman, T. E. King, A. Pardo; American Thoracic Society; European Respiratory Society; American College of Chest Physicians, Idiopathic pulmonary fibrosis: Prevailing and evolving hypotheses about its pathogenesis and implications for therapy. *Ann. Intern. Med.* **134**, 136–151 (2001).
2. V. J. Thannickal, G. B. Toews, E. S. White, J. P. Lynch III, F. J. Martinez, Mechanisms of pulmonary fibrosis. *Annu. Rev. Med.* **55**, 395–417 (2004).
3. D. Behera, S. Kaur, G. Sathyanarayana, A. Bhatnagar, S. Majumdar, Nitric oxide derivative in bronchoalveolar lavage fluid from patients with idiopathic pulmonary fibrosis. *Indian J. Chest Dis. Allied Sci.* **44**, 21–24 (2002).
4. C. Montaldo, E. Cannas, M. Ledda, L. Rosetti, L. Congiu, L. Atzori, Bronchoalveolar glutathione and nitrite/nitrate in idiopathic pulmonary fibrosis and sarcoidosis. *Sarcoidosis Vasc. Diffuse Lung Dis.* **19**, 54–58 (2002).
5. D. Saleh, P. J. Barnes, A. Giaid, Increased production of the potent oxidant peroxynitrite in the lungs of patients with idiopathic pulmonary fibrosis. *Am. J. Respir. Crit. Care Med.* **155**, 1763–1769 (1997).
6. X. L. Chen, W. B. Li, A. M. Zhou, J. Ai, S. S. Huang, Role of endogenous peroxynitrite in pulmonary injury and fibrosis induced by bleomycin A5 in rats. *Acta Pharmacol. Sin.* **24**, 697–702 (2003).
7. A. S. Jang, J. U. Lee, I. S. Choi, K. O. Park, J. H. Lee, S. W. Park, C. S. Park, Expression of nitric oxide synthase, aquaporin 1 and aquaporin 5 in rat after bleomycin inhalation. *Intensive Care Med.* **30**, 489–495 (2004).
8. T. Ogawa, M. Kimoto, K. Sasaoka, Occurrence of a new enzyme catalyzing the direct conversion of N^G,N^G-dimethyl-L-arginine to L-citrulline in rats. *Biochem. Biophys. Res. Commun.* **148**, 671–677 (1987).
9. J. M. Leiper, J. Santa Maria, A. Chubb, R. J. MacAllister, I. G. Charles, G. S. Whitley, P. Vallance, Identification of two human dimethylarginine dimethylaminohydrolases with distinct tissue distributions and homology with microbial arginine deiminases. *Biochem. J.* **343** (Pt 1), 209–214 (1999).
10. A. E. McBride, P. A. Silver, State of the Arg: Protein methylation at arginine comes of age. *Cell* **106**, 5–8 (2001).
11. P. Vallance, A. Leone, A. Calver, J. Collier, S. Moncada, Accumulation of an endogenous inhibitor of nitric oxide synthesis in chronic renal failure. *Lancet* **339**, 572–575 (1992).
12. D. J. Jiang, S. J. Jia, Z. Dai, Y. J. Li, Asymmetric dimethylarginine induces apoptosis via p38 MAPK/caspase-3-dependent signaling pathway in endothelial cells. *J. Mol. Cell. Cardiol.* **40**, 529–539 (2006).
13. J. L. Jiang, S. Wang, N. S. Li, X. H. Zhang, H. W. Deng, Y. J. Li, The inhibitory effect of simvastatin on the ADMA-induced inflammatory reaction is mediated by MAPK pathways in endothelial cells. *Biochem. Cell Biol.* **85**, 66–77 (2007).
14. H. Dayoub, V. Achan, S. Adimoolam, J. Jacobi, M. C. Stuehlinger, B. Y. Wang, P. S. Tsao, M. Kimoto, P. Vallance, A. J. Patterson, J. P. Cooke, Dimethylarginine dimethylaminohydrolase regulates nitric oxide synthesis: Genetic and physiological evidence. *Circulation* **108**, 3042–3047 (2003).
15. S. Pullamsetti, L. Kiss, H. A. Ghofrani, R. Voswinckel, P. Haredza, W. Klepetko, C. Aigner, L. Fink, J. P. Muyal, N. Weissmann, F. Grimminger, W. Seeger, R. T. Schermuly, Increased levels and reduced catabolism of asymmetric and symmetric dimethylarginines in pulmonary hypertension. *FASEB J.* **19**, 1175–1177 (2005).
16. J. Leiper, M. Nandi, B. Torondel, J. Murray-Rust, M. Malaki, B. O'Hara, S. Rossiter, S. Anthony, M. Madhani, D. Selwood, C. Smith, B. Wojciak-Stothard, A. Rudiger, R. Stidwill, N. Q. McDonald, P. Vallance, Disruption of methylarginine metabolism impairs vascular homeostasis. *Nat. Med.* **13**, 198–203 (2007).
17. H. Konishi, K. Sydow, J. P. Cooke, Dimethylarginine dimethylaminohydrolase promotes endothelial repair after vascular injury. *J. Am. Coll. Cardiol.* **49**, 1099–1105 (2007).
18. W. S. el-Deiry, p21/p53, cellular growth control and genomic integrity. *Curr. Top. Microbiol. Immunol.* **227**, 121–137 (1998).
19. S. L. Harris, A. J. Levine, The p53 pathway: Positive and negative feedback loops. *Oncogene* **24**, 2899–2908 (2005).
20. H. R. Collard, T. E. King Jr., Demystifying idiopathic interstitial pneumonia. *Arch. Intern. Med.* **163**, 17–29 (2003).
21. G. Raghu, K. K. Brown, W. Z. Bradford, K. Starko, P. W. Noble, D. A. Schwartz, T. E. King Jr.; Idiopathic Pulmonary Fibrosis Study Group, A placebo-controlled trial of interferon γ-1b in patients with idiopathic pulmonary fibrosis. *N. Engl. J. Med.* **350**, 125–133 (2004).
22. A. Azuma, T. Nukiwa, E. Tsuboi, M. Suga, S. Abe, K. Nakata, Y. Taguchi, S. Nagai, H. Itoh, M. Ohi, A. Sato, S. Kudoh, Double-blind, placebo-controlled trial of pirfenidone in patients with idiopathic pulmonary fibrosis. *Am. J. Respir. Crit. Care Med.* **171**, 1040–1047 (2005).
23. T. E. King Jr., J. Behr, K. K. Brown, R. M. du Bois, L. Lancaster, J. A. de Andrade, G. Stähler, I. Leconte, S. Roux, G. Raghu, BUILD-1: A randomized placebo-controlled trial of bosentan in idiopathic pulmonary fibrosis. *Am. J. Respir. Crit. Care Med.* **177**, 75–81 (2008).
24. M. Demedts, J. Behr, R. Buhl, U. Costabel, R. Dekhuijzen, H. M. Jansen, W. MacNee, M. Thomeer, B. Wallaert, F. Laurent, A. G. Nicholson, E. K. Verbeken, J. Verschakelen, C. D. Flower, F. Capron, S. Petruzzelli, P. De Vuyst, J. M. van den Bosch, E. Rodriguez-Becerra, G. Corvasce, I. Lankhorst, M. Sardina, M. Montanari; IFIGENIA Study Group, High-dose acetylcysteine in idiopathic pulmonary fibrosis. *N. Engl. J. Med.* **353**, 2229–2242 (2005).
25. R. H. Böger, J. P. Cooke, P. Vallance, ADMA: An emerging cardiovascular risk factor. *Vasc. Med.* **10** (Suppl. 1), S1–S2 (2005).
26. V. Bermúdez, F. Bermúdez, G. Acosta, A. Acosta, J. Añez, C. Andara, E. Leal, C. Cano, V. Manuel, R. Hernández, Z. Israili, Molecular mechanisms of endothelial dysfunction: From nitric oxide synthesis to ADMA inhibition. *Am. J. Ther.* **15**, 326–333 (2008).
27. A. Schwentker, Y. Vodovotz, R. Weller, T. R. Billiar, Nitric oxide and wound repair: Role of cytokines? *Nitric Oxide* **7**, 1–10 (2002).
28. N. Petrova, M. Edmonds, Emerging drugs for diabetic foot ulcers. *Expert Opin. Emerg. Drugs* **11**, 709–724 (2006).
29. M. G. Ferrini, D. Vernet, T. R. Magee, A. Shahed, A. Qian, J. Rajfer, N. F. Gonzalez-Cadavid, Antifibrotic role of inducible nitric oxide synthase. *Nitric Oxide* **6**, 283–294 (2002).
30. T. Geiser, Idiopathic pulmonary fibrosis—a disorder of alveolar wound repair? *Swiss Med. Wkly.* **133**, 405–411 (2003).
31. R. C. Chambers, Procoagulant signalling mechanisms in lung inflammation and fibrosis: Novel opportunities for pharmacological intervention? *Br. J. Pharmacol.* **153** (Suppl. 1), S367–S378 (2008).
32. S. Ueda, S. Kato, H. Matsuoka, M. Kimoto, S. Okuda, M. Morimatsu, T. Imaizumi, Regulation of cytokine-induced nitric oxide synthesis by asymmetric dimethylarginine: Role of dimethylarginine dimethylaminohydrolase. *Circ. Res.* **92**, 226–233 (2003).
33. J. Gauldie, P. J. Sime, Z. Xing, B. Marr, G. M. Tremblay, Transforming growth factor-β gene transfer to the lung induces myofibroblast presence and pulmonary fibrosis. *Curr. Top. Pathol.* **93**, 35–45 (1999).
34. I. Shahar, E. Fireman, M. Topilsky, J. Grief, S. Kivity, Z. Spirer, S. Ben Efraim, Effect of IL-6 on alveolar fibroblast proliferation in interstitial lung diseases. *Clin. Immunol. Immunopathol.* **79**, 244–251 (1996).
35. J. Jacobi, K. Sydow, G. von Degenfeld, Y. Zhang, H. Dayoub, B. Wang, A. J. Patterson, M. Kimoto, H. M. Blau, J. P. Cooke, Overexpression of dimethylarginine dimethylaminohydrolase reduces tissue asymmetric dimethylarginine levels and enhances angiogenesis. *Circulation* **111**, 1431–1438 (2005).
36. J. J. Coalson, The ultrastructure of human fibrosing alveolitis. *Virchows Arch. A Pathol. Anat. Histol.* **395**, 181–199 (1982).
37. B. Corrin, A. Dewar, Pathogenesis of idiopathic interstitial pulmonary fibrosis. *Ultrastruct. Pathol.* **20**, 369–371 (1996).
38. M. Gharaee-Kermani, M. Ullenbruch, S. H. Phan, Animal models of pulmonary fibrosis. *Methods Mol. Med.* **117**, 251–259 (2005).

39. C. G. Lee, H. R. Kang, R. J. Homer, G. Chupp, J. A. Elias, Transgenic modeling of transforming growth factor-β_1: Role of apoptosis in fibrosis and alveolar remodeling. *Proc. Am. Thorac. Soc.* **3**, 418–423 (2006).
40. K. Kuwano, N. Hagimoto, M. Kawasaki, T. Yatomi, N. Nakamura, S. Nagata, T. Suda, R. Kunitake, T. Maeyama, H. Miyazaki, N. Hara, Essential roles of the Fas-Fas ligand pathway in the development of pulmonary fibrosis. *J. Clin. Invest.* **104**, 13–19 (1999).
41. M. Konigshoff, M. Kramer, N. Balsara, J. Wilhelm, O. V. Amarie, A. Jahn, F. Rose, L. Fink, W. Seeger, L. Schaefer, A. Günther, O. Eickelberg, WNT1-inducible signaling protein–1 mediates pulmonary fibrosis in mice and is upregulated in humans with idiopathic pulmonary fibrosis. *J. Clin. Invest.* **119**, 772–787 (2009).
42. A. L. Degryse, H. Tanjore, X. C. Xu, V. V. Polosukhin, B. R. Jones, F. B. McMahon, L. A. Gleaves, T. S. Blackwell, W. E. Lawson, Repetitive intratracheal bleomycin models several features of idiopathic pulmonary fibrosis. *Am. J. Physiol. Lung Cell. Mol. Physiol.* **299**, L442–L452 (2010).
43. K. K. Kim, M. C. Kugler, P. J. Wolters, L. Robillard, M. G. Galvez, A. N. Brumwell, D. Sheppard, H. A. Chapman, Alveolar epithelial cell mesenchymal transition develops in vivo during pulmonary fibrosis and is regulated by the extracellular matrix. *Proc. Natl. Acad. Sci. U.S.A.* **103**, 13180–13185 (2006).
44. H. Tanjore, X. C. Xu, V. V. Polosukhin, A. L. Degryse, B. Li, W. Han, T. P. Sherrill, D. Plieth, E. G. Neilson, T. S. Blackwell, W. E. Lawson, Contribution of epithelial-derived fibroblasts to bleomycin-induced lung fibrosis. *Am. J. Respir. Crit. Care Med.* **180**, 657–665 (2009).
45. K. Hasegawa, S. Wakino, T. Tanaka, M. Kimoto, S. Tatematsu, T. Kanda, K. Yoshioka, K. Homma, N. Sugano, M. Kurabayashi, T. Saruta, K. Hayashi, Dimethylarginine dimethylaminohydrolase 2 increases vascular endothelial growth factor expression through Sp1 transcription factor in endothelial cells. *Arterioscler. Thromb. Vasc. Biol.* **26**, 1488–1494 (2006).
46. D. Wang, P. S. Gill, T. Chabrashvili, M. L. Onozato, J. Raggio, M. Mendonca, K. Dennehy, M. Li, P. Modlinger, J. Leiper, P. Vallance, O. Adler, A. Leone, A. Tojo, W. J. Welch, C. S. Wilcox, Isoform-specific regulation by N^G,N^G-dimethylarginine dimethylaminohydrolase of rat serum asymmetric dimethylarginine and vascular endothelium-derived relaxing factor/NO. *Circ. Res.* **101**, 627–635 (2007).
47. T. Genovese, S. Cuzzocrea, R. Di Paola, M. Failla, E. Mazzon, M. A. Sortino, G. Frasca, E. Gili, N. Crimi, A. P. Caputi, C. Vancheri, Inhibition or knock out of inducible nitric oxide synthase result in resistance to bleomycin-induced lung injury. *Respir. Res.* **6**, 58 (2005).
48. B. W. Kinder, K. K. Brown, M. I. Schwarz, J. H. Ix, A. Kervitsky, T. E. King Jr., Baseline BAL neutrophilia predicts early mortality in idiopathic pulmonary fibrosis. *Chest* **133**, 226–232 (2008).
49. M. S. Wilson, S. K. Madala, T. R. Ramalingam, B. R. Gochuico, I. O. Rosas, A. W. Cheever, T. A. Wynn, Bleomycin and IL-1β–mediated pulmonary fibrosis is IL-17A dependent. *J. Exp. Med.* **207**, 535–552 (2010).
50. S. Cook, P. Vollenweider, B. Ménard, M. Egli, P. Nicod, U. Scherrer, Increased eNO and pulmonary iNOS expression in eNOS null mice. *Eur. Respir. J.* **21**, 770–773 (2003).
51. K. Hasegawa, S. Wakino, T. Tanaka, M. Kimoto, S. Tatematsu, T. Kanda, K. Yoshioka, K. Homma, N. Sugano, M. Kurabayashi, T. Saruta, K. Hayashi, Dimethylarginine dimethylaminohydrolase 2 increases vascular endothelial growth factor expression through Sp1 transcription factor in endothelial cells. *Arterioscler. Thromb. Vasc. Biol.* **26**, 1488–1494 (2006).
52. M. Myllärniemi, P. Lindholm, M. J. Ryynänen, C. R. Kliment, K. Salmenkivi, J. Keski-Oja, V. L. Kinnula, T. D. Oury, K. Koli, Gremlin-mediated decrease in bone morphogenetic protein signaling promotes pulmonary fibrosis. *Am. J. Respir. Crit. Care Med.* **177**, 321–329 (2008).
53. American Thoracic Society; European Respiratory Society, American Thoracic Society/European Respiratory Society International Multidisciplinary Consensus Classification of the Idiopathic Interstitial Pneumonias. This joint statement of the American Thoracic Society (ATS), and the European Respiratory Society (ERS) was adopted by the ATS board of directors, June 2001 and by the ERS Executive Committee, June 2001. *Am. J. Respir. Crit. Care Med.* **165**, 277–304 (2002).
54. T. Ashcroft, J. M. Simpson, V. Timbrell, Simple method of estimating severity of pulmonary fibrosis on a numerical scale. *J. Clin. Pathol.* **41**, 467–470 (1988).
55. R. T. Schermuly, S. S. Pullamsetti, G. Kwapiszewska, R. Dumitrascu, X. Tian, N. Weissmann, H. A. Ghofrani, C. Kaulen, T. Dunkern, C. Schudt, R. Voswinckel, J. Zhou, A. Samidurai, W. Klepetko, R. Paddenberg, W. Kummer, W. Seeger, F. Grimminger, Phosphodiesterase 1 upregulation in pulmonary arterial hypertension: Target for reverse-remodeling therapy. *Circulation* **115**, 2331–2339 (2007).
56. T. López-Rovira, E. Chalaux, J. Massagué, J. L. Rosa, F. Ventura, Direct binding of Smad1 and Smad4 to two distinct motifs mediates bone morphogenetic protein-specific transcriptional activation of Id1 gene. *J. Biol. Chem.* **277**, 3176–3185 (2002).

57. **Acknowledgments:** We thank S. Ficus, K. Wiedl, and M. Hoeck for their technical assistance. **Funding:** Supported by German Research Council KFO 118 "Pathomechanisms and Therapy of Lung Fibrosis," Excellence Cluster Cardio Pulmonary System, European Commission under the Sixth Framework Programme (contract no. LSHM-CT-2005-018725, PULMOTENSION), The Else-Kröner-Fresenius Foundation, The British Heart Foundation (J.L.), and The Wellcome Trust (J.L.). **Author contributions:** S.S.P. designed and performed the experiments, analyzed the data, and wrote the manuscript. R.S., R.D., B.K.D., J.W., M.K., and D.Z. performed the experiments. H.A.G., N.W., O.E., A.G., J.L., F.G., and W.S. contributed materials and edited the manuscript. R.T.S. was awarded funding to support the study and wrote the manuscript. **Competing interests:** J.L. is an inventor on a patent filed by the University College London relating to inhibitors of DDAH1. O.E. is a scientific consultant on tissue fibrosis to Roche; A.G. is a scientific consultant to Pfizer, Intermune, and Nycomed. The other authors declare that they have no competing interests.

Submitted 20 September 2010
Accepted 16 May 2011
Published 15 June 2011
10.1126/scitranslmed.3001725

Citation: S. S. Pullamsetti, R. Savai, R. Dumitrascu, B. K. Dahal, J. Wilhelm, M. Konigshoff, D. Zakrzewicz, H. A. Ghofrani, N. Weissmann, O. Eickelberg, A. Guenther, J. Leiper, W. Seeger, F. Grimminger, R. T. Schermuly, The role of dimethylarginine dimethylaminohydrolase in idiopathic pulmonary fibrosis. *Sci. Transl. Med.* **3**, 87ra53 (2011).

INTERSTITIAL LUNG DISEASE

Autoimmune Attack Takes Your Breath Away

Tamsin M. Lindstrom[1] and William H. Robinson[1,2]*

Autoimmune targeting of a lung-specific protein can cause interstitial lung disease (Shum *et al.*, this issue).

How to best manage interstitial lung disease (ILD) is a contentious issue, one involving multidisciplinary, and often divisive, discussion between pulmonologists, rheumatologists, and radiologists. This is because the cause of ILD—a diverse group of disorders in which the connective tissue of the lungs becomes inflamed and fibrotic—is often unclear and its different forms ill-defined (*1*). Some forms of ILD are relatively straightforward, arising from an infection or from exposure to certain drugs or hazardous materials. Other forms are known to develop in association with autoimmune diseases called connective tissue disorders (CTDs), yet their precise etiology remains elusive. Even more perplexing are the ILD forms deemed idiopathic, although these cases sometimes turn out to be an early manifestation of CTD-associated ILD (CTD-ILD). Because CTD-ILD occurs in the setting of systemic autoimmunity, and even idiopathic ILD may be associated with signs of autoimmunity, there has been much debate about a possible role for autoimmunity in the pathogenesis of ILD (*1*–*7*). But no autoimmune mechanism has been evinced—until now. In this issue of *Science Translational Medicine*, Shum and colleagues (*8*) show that in a subset of CTD-ILD and idiopathic-ILD cases, autoimmune targeting of a lung-specific protein may be at the root of the disease.

A LUNG-SPECIFIC AUTOANTIGEN

Indirect evidence for an autoimmune etiology of ILD has come from the detection of immune-cell infiltrates in the lungs and autoantibodies in the blood and bronchoalveolar lavage fluid, not only in CTD-ILD but surprisingly also in idiopathic ILD (*1*–*6*). Moreover, in idiopathic ILD certain autoantibodies appear to be associated with more severe disease (*6*) or with acute exacerbation of disease (*4*). However, none of these autoantibodies targets lung-specific proteins, so it is unclear (i) whether their presence simply reflects the systemic autoimmunity underlying the associated CTD in CTD-ILD and (ii) how they could cause disease that is limited to the lungs in idiopathic ILD. Some insight into this conundrum might be gleaned from studies on lung disease that develops in patients with autoimmune polyendocrine syndrome type 1 (APS1), a rare autoimmune disorder. Alimohammadi *et al.* (*9*) showed that APS1 patients with respiratory symptoms have autoantibodies to KCNRG, a potassium channel–regulating protein preferentially expressed in the bronchiolar epithelium. Finding that loss of immune tolerance to BPIFB9 (also known as vomeromodulin) can cause ILD-like lung pathology in mice, Shum *et al.* (*7*) used this information to identify autoantibodies to the related lung-specific protein BPIFB1 (BPIFB9 is a pseudogene in humans) in a patient with APS1-ILD.

In this issue of *Science Translational Medicine*, Shum *et al.* (*8*) broaden their scope, shedding light on the relevance of autoimmunity to the pathogenesis of the more common and inscrutable forms of ILD. They started once more by studying APS1-ILD but then extended their findings to CTD-ILD and idiopathic ILD. Because APS1 involves production of autoantibodies to organ-specific antigens and is a well-characterized monogenic disorder caused by defects in the *autoimmune regulator* (*AIRE*) gene, the authors reasoned that studying autoimmune responses in patients with APS1, as well as in mice with an equivalent defect in *Aire*, would yield mechanistic insights into the pathogenesis of ILD that have so far been lacking—and, importantly, answer the question of whether autoimmunity can cause ILD.

The authors previously detected autoantibodies to BPIFB1 in the blood of a single APS1 patient (*7*). In the new study (*8*), they screened a large cohort ($n = 104$) of APS1 patients with and without ILD and found that BPIFB1 autoantibodies were present in the blood of only a small proportion of the total cohort of APS1 patients but were present in all six of the APS1 patients with ILD. Shum and colleagues then showed that expression of human BPIFB1 is restricted to the lungs and thymus. This expression pattern is telling because the way in which AIRE promotes immune tolerance is by orchestrating the ectopic expression of tissue-specific antigens in the thymus, brokering an encounter between them and maturing T cells; this process—called central tolerance—results in the purging of potentially dangerous T cells that react too strongly with these antigens (*10*). These new findings (*8*) suggest that BPIFB1 is a lung-specific protein that normally enjoys AIRE-mediated protection from autoimmune attack, protection that is compromised in APS1. Indeed, in immunofluorescence experiments, antibodies in APS1-ILD serum bound to BPIFB1 present in human bronchiolar epithelium (Fig. 1). Together, these findings identify BPIFB1 as a lung-specific autoantigen in APS1-ILD.

The authors next showed that BPIFB1 autoantibodies were also present in a subset of patients with CTD-associated ILD—and even in a subset of patients with idiopathic ILD (Fig. 1) (*8*). These autoantibodies were not present in healthy individuals, nor in patients with type I diabetes, an autoimmune disorder that does not feature lung pathology—indicating that the autoantibodies are not simply a general biomarker of systemic autoimmunity but rather an indicator of lung-specific autoimmunity in diverse types of ILD.

PROVING CAUSATION

Yet, association does not prove causation. To demonstrate that autoimmune targeting of a BPIFB protein is not only associated with ILD but can actually cause it, Shum *et al.* (*8*) performed mechanistic experiments with the *Aire*$^{-/-}$ mouse model of APS1. They showed that autoantibodies to BPIFB9 [previously identified as a lung-specific autoantigen in mice (*7*)] served as molecular indicators of the presence and severity of lung disease in *Aire*$^{-/-}$ mice. In some diseases, autoantibodies can themselves inflict damage, whereas in others, they are an epiphenomenon of pathogenic T cell responses elicited by the same autoantigen. In this case, it was BPIFB9-specific CD4$^+$ T cells, rather than the autoantibodies to BPIFB9, that caused ILD when transferred to immunodeficient mice. Thymic transplantation experiments

[1]Division of Immunology and Rheumatology, Department of Medicine, Stanford University School of Medicine, CCSR, 269 Campus Drive, Stanford, CA 94305, USA. [2]VA Palo Alto Health Care System, Geriatric Research Education and Clinical Center, MC 154R, 3801 Miranda Avenue, Palo Alto, CA 94304, USA.
*Corresponding author. E-mail: wrobins@stanford.edu

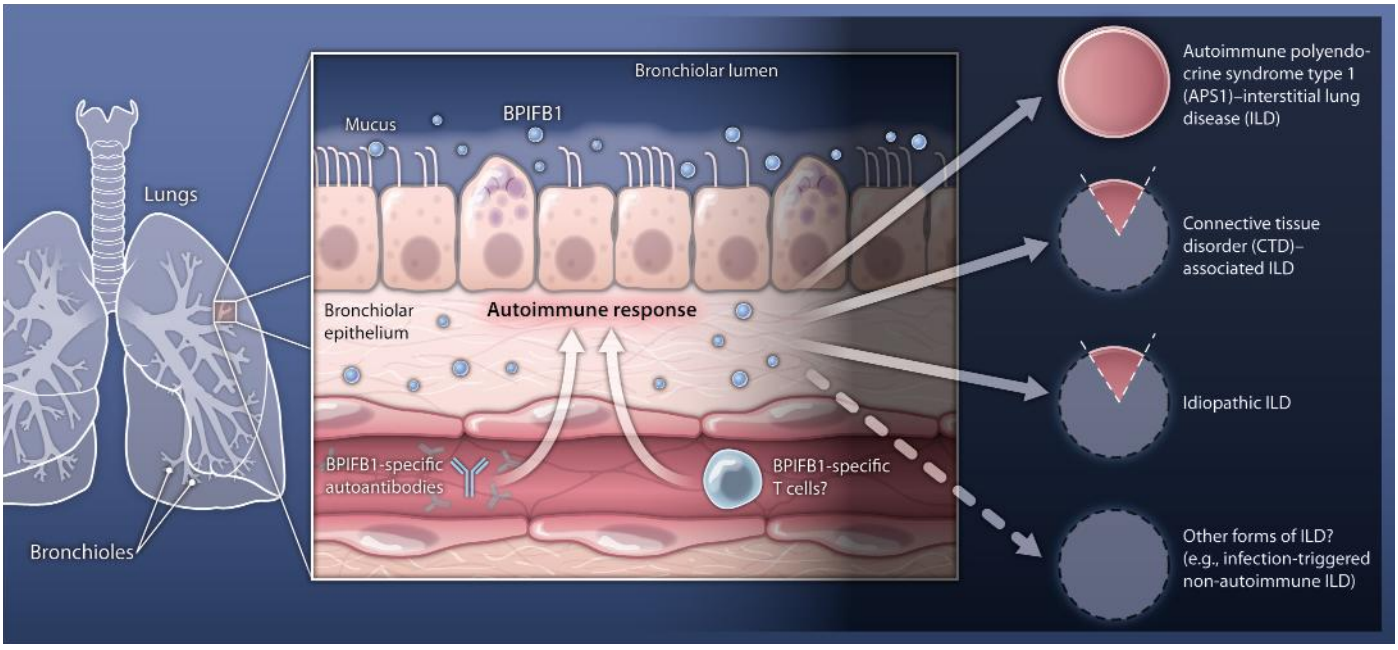

Fig. 1. Friendly fire causes lung disease. Autoimmune targeting of BPIFB1, a lung-specific protein expressed by the bronchiolar epithelium, causes APS1-associated ILD, as well as a proportion of CTD-associated and "idiopathic" cases of ILD. Loss of tolerance to BPIFB1 results in targeting of BPIFB1 by both autoantibodies and autoreactive T cells, with the T cells most likely being the perpetrators of lung damage. This new knowledge could pave the way for autoantibody-based tests and immunomodulatory treatments for autoimmune-driven ILD.

showed that BPIFB9-specific autoimmunity and lung disease developed in mice with *Aire*$^{-/-}$ thymi but not in those with *Aire*$^{+/-}$ thymi, confirming that defects in central tolerance to a lung antigen can cause ILD.

However, it is BPIFB1, not BPIFB9, that is targeted in human ILD, and most cases of ILD—those not linked to APS1—are not associated with a known defect in *AIRE*. Shum *et al.* (*8*) therefore used a different mouse model to determine whether a break in tolerance could result in BPIFB1 targeting and, hence, ILD. Because *Bpifb1*$^{-/-}$ mice have not previously encountered BPIFB1, they have not developed immune tolerance to this protein, so that immunization of these mice with BPIFB1 induces anti-BPIFB1 immune responses. Transfer of BPIFB1-specific lymphocytes from BPIFB1-immunized *Bpifb1*$^{-/-}$ mice to lymphocyte-deficient *Bpifb1*$^{+/+}$ mice induced ILD in the recipient mice, indicating that autoimmune targeting of BPIFB1—independent of a defect in *Aire*—can also cause ILD.

QUESTIONS AND CLINICAL IMPLICATIONS

Thus, by using a well-characterized but rare disorder as a starting point, Shum *et al.* (*8*) demonstrated that lung-specific autoimmunity may cause ILD associated with more common diseases, as well as ILD so far deemed idiopathic. This exciting finding increases our understanding of ILD and raises a slew of questions:

How do the autoantibodies to BPIFB1 arise in CTD-ILD and idiopathic ILD? Do they arise as a result of unknown *AIRE* defects that are subtler than those in APS1, or as a result of *AIRE*-independent defects in peripheral tolerance (which complements central tolerance), or both? With this in mind, do *Aire*$^{-/-}$ mice with ILD develop autoantibodies to BPIFB1, in addition to autoantibodies to BPIFB9? Do ILD patients with autoantibodies to BPIFB1 have BPIFB1-specific T cells in their lungs? What is the relationship between autoantibodies to BPIFB1 and the other ILD-associated autoantibodies identified, especially the lung-specific autoantigen KCNRG (9)? Are they present in the same or in distinct patient subsets? What causes CTD-ILD and idiopathic ILD in patients who do not have autoantibodies to BPIFB1? Is the ILD of autoimmune origin in these patients as well, involving targeting of a different lung autoantigen, or is it not autoimmune but rather the result of unrecognized exposures or other factors? Might autoimmunity even contribute to yet other forms of ILD? For example, in infection-triggered ILD, protective immune responses could conceivably segue to pathogenic autoimmune responses through cross-reactivity. What other so-called idiopathic diseases might in fact be autoimmune in origin?

The findings also have important implications for disease management. Although it remains to be tested in an independent patient cohort, the ability of autoantibodies to BPIFB1 to identify autoimmune-driven ILD could prove transformative. A biomarker enabling identification of individuals whose ILD is of autoimmune origin would allow more effective management of their pulmonary disease, by indicating the need for immunomodulatory treatment. Indeed, idiopathic ILD has, in general, a worse prognosis than CTD-ILD, possibly because individuals with CTD-ILD are more likely to be treated with immunosuppressive drugs (aimed at tackling the autoimmunity underlying CTDs) (*1*). Perhaps autoantibodies to BPIFB1 will also prove useful as biomarkers that predict the onset or progression of ILD, which would allow for preventive interventions. Moreover, if BPIFB1 is indeed a critical lung autoantigen, development of antigen-specific tolerizing therapies for autoimmune ILD becomes a possibility. Even if the promise of biomarker tests and tolerizing therapies based on BPIFB1 is not borne out, the find-

ings by Shum *et al.* substantiate the idea that lung-directed autoimmunity can cause ILD. Thus, the stage is set for further dissection of the role of autoimmunity and the benefit of immunomodulatory treatment in ILD, as well as the classification of ILD on the basis of mechanism rather than association.

REFERENCES AND NOTES

1. A. Fischer, R. du Bois, Interstitial lung disease in connective tissue disorders. *Lancet* **380**, 689–698 (2012).
2. J. Fujita, N. Dobashi, Y. Ohtsuki, I. Yamadori, T. Yoshinouchi, T. Kamei, M. Tokuda, S. Hojo, H. Okada, J. Takahara, Elevation of anti-cytokeratin 19 antibody in sera of the patients with idiopathic pulmonary fibrosis and pulmonary fibrosis associated with collagen vascular disorders. *Lung* **177**, 311–319 (1999).
3. K. A. Keogh, A. H. Limper, Characterization of lymphocyte populations in nonspecific interstitial pneumonia. *Respir. Res.* **6**, 137 (2005).
4. K. Kurosu, Y. Takiguchi, O. Okada, N. Yumoto, S. Sakao, Y. Tada, Y. Kasahara, N. Tanabe, K. Tatsumi, M. Weiden, W. N. Rom, T. Kuriyama, Identification of annexin 1 as a novel autoantigen in acute exacerbation of idiopathic pulmonary fibrosis. *J. Immunol.* **181**, 756–767 (2008).
5. Y. Yang, J. Fujita, S. Bandoh, Y. Ohtsuki, I. Yamadori, T. Yoshinouchi, T. Ishida, Detection of antivimentin antibody in sera of patients with idiopathic pulmonary fibrosis and non-specific interstitial pneumonia. *Clin. Exp. Immunol.* **128**, 169–174 (2002).
6. C. Taillé, S. Grootenboer-Mignot, C. Boursier, L. Michel, M. P. Debray, J. Fagart, L. Barrientos, A. Mailleux, N. Cigna, F. Tubach, J. Marchal-Sommé, P. Soler, S. Chollet-Martin, B. Crestani, Identification of periplakin as a new target for autoreactivity in idiopathic pulmonary fibrosis. *Am. J. Respir. Crit. Care Med.* **183**, 759–766 (2011).
7. A. K. Shum, J. DeVoss, C. L. Tan, Y. Hou, K. Johannes, C. S. O'Gorman, K. D. Jones, E. B. Sochett, L. Fong, M. S. Anderson, Identification of an autoantigen demonstrates a link between interstitial lung disease and a defect in central tolerance. *Sci. Transl. Med.* **1**, 9ra20 (2009).
8. A. K. Shum, M. Alimohammadi, C. L. Tan, M. H. Cheng, T. C. Metzger, C. S. Law, W. Lwin, J. Perheentupa, H. Bour-Jordan, J. C. Carel, E. S. Husebye, F. De Luca, C. Janson, R. Sargur, N. Dubois, M. Kajosaari, P. J. Wolters, H. A. Chapman, O. Kämpe, M. S. Anderson, BPIFB1 is a lung-specific autoantigen associated with interstitial lung disease. *Sci. Transl. Med.* **5**, 206ra138 (2013).
9. M. Alimohammadi, N. Dubois, F. Sköldberg, A. Hallgren, I. Tardivel, H. Hedstrand, J. Haavik, E. S. Husebye, J. Gustafsson, F. Rorsman, A. Meloni, C. Janson, B. Vialettes, M. Kajosaari, W. Egner, R. Sargur, F. Pontén, Z. Amoura, A. Grimfeld, F. De Luca, C. Betterle, J. Perheentupa, O. Kämpe, J. C. Carel, Pulmonary autoimmunity as a feature of autoimmune polyendocrine syndrome type 1 and identification of KCNRG as a bronchial autoantigen. *Proc. Natl. Acad. Sci. U.S.A.* **106**, 4396–4401 (2009).
10. T. C. Metzger, M. S. Anderson, Control of central and peripheral tolerance by Aire. *Immunol. Rev.* **241**, 89–103 (2011).

10.1126/scitranslmed.3007233

Citation: T. M. Lindstrom, W. H. Robinson, Autoimmune attack takes your breath away. *Sci. Transl. Med.* **5**, 206fs36 (2013).

Science Translational Medicine
AAAS

The Role of Dimethylarginine Dimethylaminohydrolase in Idiopathic Pulmonary Fibrosis

Soni Savai Pullamsetti *et al.*

Sci Transl Med **3**, 87ra53 (2011);
DOI: 10.1126/scitranslmed.3001725

Editor's Summary

Matter of Life and Breath

For many, fresh air can be rejuvenating, but for patients with idiopathic pulmonary fibrosis (IPF), it can be life saving. This progressive, debilitating, and sometimes fatal disease steals breath from its victims by strangling the lungs with a buildup of excess fibrous connective tissue (scarring). No effective treatments exist to correct this poorly understood process of fibrosis in overdrive. Pullamsetti *et al*. now identify a critical enzyme, dimethylarginine dimethylaminohydrolase (DDAH), which is overly active in IPF patients' lungs and in mice with an IPF-like lung injury. Inhibition of enzyme activity attenuates many features of the disease, suggesting a new potential therapy.

The authors noted that there were especially large amounts of DDAH in cells from the lungs of IPF patients and a mouse model of IPF in which lung tissue is scarred by treatment with the antibiotic bleomycin. This enzyme breaks down an endogenous inhibitor of inducible nitric oxide synthase (iNOS) so that when DDAH increases, iNOS activity increases, giving rise to products that can contribute to fibrosis. Inhibition of DDAH in epithelial cells from the lung alveoli of IPF patients or bleomycin-treated mice prevented two hallmarks of IPF: epithelial cell overproliferation and collagen production. A third hallmark, enhanced collagen synthesis, did not depend on iNOS and instead seemed to be mediated by transforming growth factor–β (TGFβ)/SMAD. The authors extended this work by using a drug called L-291 to inhibit DDAH in bleomycin-treated mice, which were then protected from lung fibrosis.

The improper activation of fibrosis, or scarring, in IPF is in part a result of stimulation by cytokines such as TGFβ and interleukin-6, although the full extent of the control pathways remains unclear. As shown by these new results, NO, the gaseous product of iNOS, contributes to epithelial cell proliferation and TGFβ signaling to collagen manufacture. These pathways are not likely to represent the whole story of this complex disease, but the results from this study do indicate that iNOS signaling and other events downstream from DDAH are critical for the development of lung fibrosis. Keeping these players under tight control with new therapeutic agents may provide a breath of fresh air for patients with IPF.

Science Translational Medicine (print ISSN 1946-6234; online ISSN 1946-6242) is published weekly, except the last week in December, by the American Association for the Advancement of Science, 1200 New York Avenue NW, Washington, DC 20005.